Two-dimensional material

1
- Graphene
  - symmetries
  - Effective Hamiltonian

2
- Transition metal dichalcogenide
  - Berry curvature
  - Optical transitions

3
- Haldane model
  - Haldane flux
  - Berry curvature

4
- Twisted bilayer graphene

- 1947, theory of graphene by Wallace
- 1968, Mermin-Wagner theorem (no long-range order in 2D)
- 1985, discovery of bucky ball by Kroto, Smalley, and Curl (1996 Nobel prize)
- 1991, discovery of carbon nanotube by Iijima and Ichihashi.
- 2004, first graphene produced by Geim and Novoselov (2010 Nobel prize)

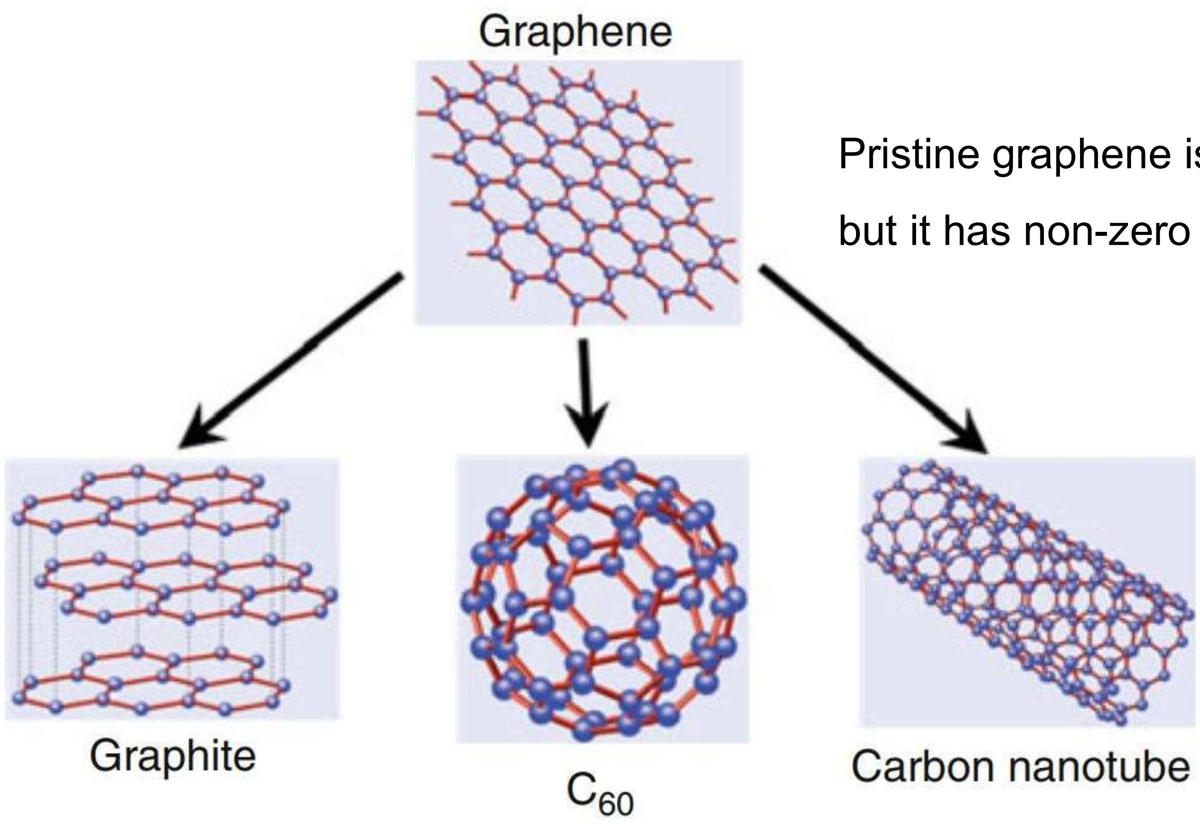

Pristine graphene is not topological,

but it has non-zero Berry curvature.

Extraordinary Properties of Graphene

- **Room-temperature electron mobility of 2.5×10^5 cm^2V^{-1} s^{-1}**

  Nano Lett. 11, 2396–2399 (2011).

- **Young's modulus of 1 TPa and intrinsic strength of 130 Gpa, the strongest materials ever tested.**

  Cu: 0.117 TPa — Phys. Rev. B 76, 064120 (2007).

- **High thermal conductivity: above 3,000 $Wm^{-1}K^{-1}$**

  Cu: 401 $Wm^{-1}K^{-1}$ — Nature Mater. 10, 569–581 (2011).

- **A prediction in 2015 suggested a melting point at least 5000 K.**

- **Optical absorption of 2.3%**

  Science 320, 1308 (2008).

- **No band gap for undoped graphene**

- **The electrical resistivity of graphene < 10^{-6} $\Omega\cdot$cm, less than silver, the lowest known at RT.**

From Raynien Kwo's ppt

1 Graphene lattice

(a)

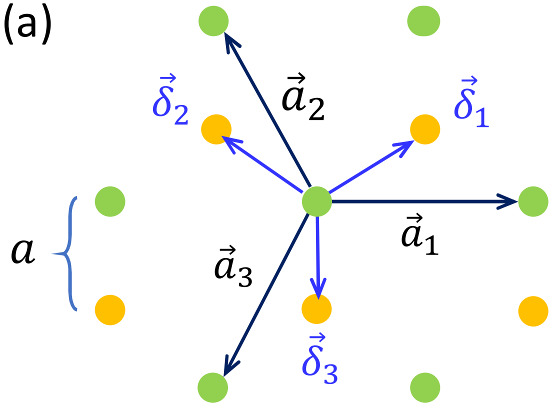

(b)

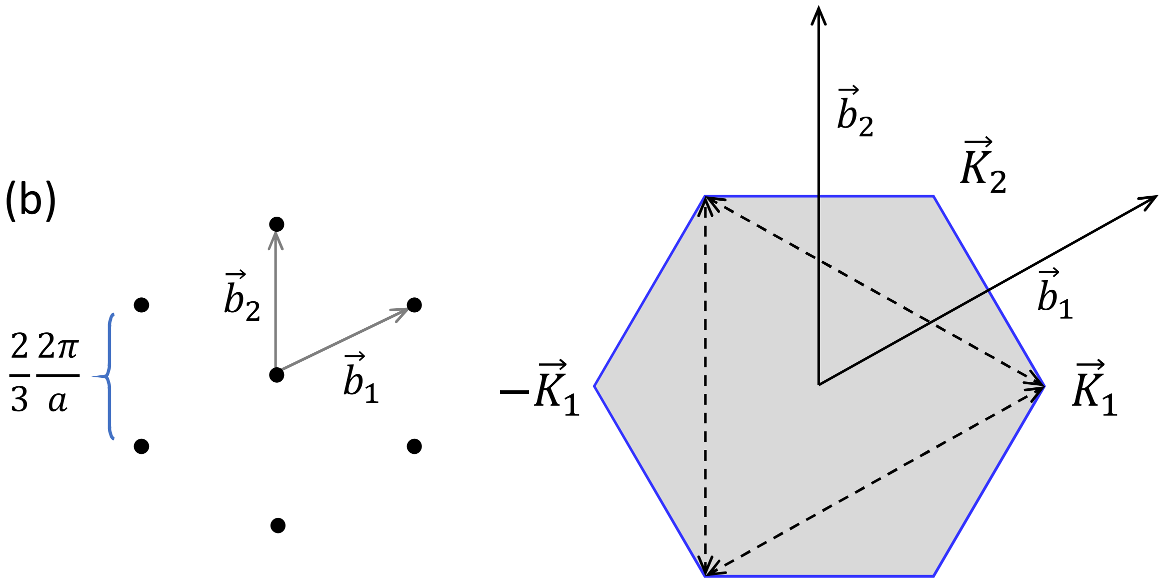

Brillouin zone

- Lattice vectors

$$
\begin{aligned}
\mathbf{a}_1 &= \sqrt{3}a\hat{x}, \\
\mathbf{a}_2 &= -\frac{\sqrt{3}}{2}a\hat{x} + \frac{3}{2}a\hat{y}, \\
\mathbf{a}_3 &= -\frac{\sqrt{3}}{2}a\hat{x} - \frac{3}{2}a\hat{y}.
\end{aligned}
$$

$$a = 1.42\ A$$

$$a_0 = \sqrt{3}a \simeq 2.46\text{Å}$$

- Reciprocal lattice vectors

$$
\begin{aligned}
\mathbf{b}_1 &= \frac{2\pi}{a}\left(\frac{2}{\sqrt{3}}\hat{x} + \frac{1}{3}\hat{y}\right), \\
\mathbf{b}_2 &= \frac{2\pi}{a}\frac{2}{3}\hat{y}.
\end{aligned}
$$

Tight-binding model
(spin neglected)

$$\hat{H} = \hat{H}_{NN} + \hat{H}_{NNN} + \hat{H}_{on-site}.$$

(1)

$$\hat{H}_{NN} = t_1 \sum_{\mathbf{R}} \left(d^\dagger_{\mathbf{R}+\boldsymbol{\delta}_1} c_{\mathbf{R}} + d^\dagger_{\mathbf{R}+\boldsymbol{\delta}_2} c_{\mathbf{R}} + d^\dagger_{\mathbf{R}+\boldsymbol{\delta}_3} c_{\mathbf{R}} \right) + h.c.$$

$$\boxed{\begin{aligned} \boldsymbol{\delta}_1 &= \frac{\sqrt{3}}{2} a\hat{x} + \frac{1}{2} a\hat{y}, \\ \boldsymbol{\delta}_2 &= -\frac{\sqrt{3}}{2} a\hat{x} + \frac{1}{2} a\hat{y}, \\ \boldsymbol{\delta}_3 &= -a\hat{y}. \end{aligned}}$$

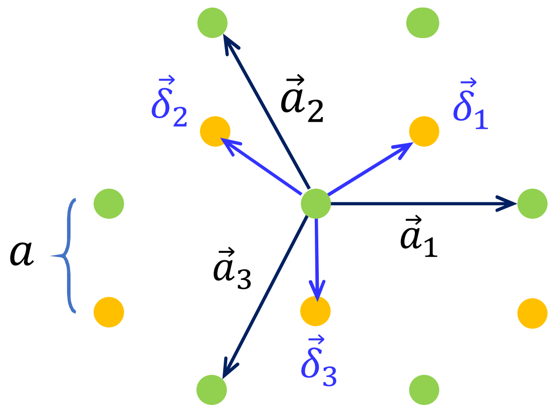

$t_1 \simeq 2.7$ eV

(2)

$$\begin{aligned} \hat{H}_{NNN} &= t_2 \sum_{\mathbf{R}} \left(c^\dagger_{\mathbf{R}+\mathbf{a}_1} c_{\mathbf{R}} + c^\dagger_{\mathbf{R}+\mathbf{a}_2} c_{\mathbf{R}} + c^\dagger_{\mathbf{R}+\mathbf{a}_3} c_{\mathbf{R}} \right) \\ &+ t_2 \sum_{\mathbf{R}} \left(d^\dagger_{\mathbf{R}+\boldsymbol{\delta}_1+\mathbf{a}_1} d_{\mathbf{R}+\boldsymbol{\delta}_1} + d^\dagger_{\mathbf{R}+\boldsymbol{\delta}_1+\mathbf{a}_2} d_{\mathbf{R}+\boldsymbol{\delta}_1} \right. \\ &\qquad \left. + d^\dagger_{\mathbf{R}+\boldsymbol{\delta}_1+\mathbf{a}_3} d_{\mathbf{R}+\boldsymbol{\delta}_1} \right) + h.c., \end{aligned}$$

(3)

$$\hat{H}_{on-site} = \Delta \sum_{\mathbf{R}} c^\dagger_{\mathbf{R}} c_{\mathbf{R}} - \Delta \sum_{\mathbf{R}} d^\dagger_{\mathbf{R}+\boldsymbol{\delta}_1} d_{\mathbf{R}+\boldsymbol{\delta}_1}$$

Fourier transform

$$\boxed{\begin{aligned} c_{\mathbf{R}} &= \frac{1}{\sqrt{N}}\sum_{\mathbf{k}} e^{i\mathbf{k}\cdot\mathbf{R}} c_{\mathbf{k}} \\ d_{\mathbf{R}+\boldsymbol{\delta}_1} &= \frac{1}{\sqrt{N}}\sum_{\mathbf{k}} e^{i\mathbf{k}\cdot(\mathbf{R}+\boldsymbol{\delta}_1)} d_{\mathbf{k}} \end{aligned}}$$

e.g.,
$$\begin{aligned} \sum_{\mathbf{R}} d^{\dagger}_{\mathbf{R}+\boldsymbol{\delta}_1} c_{\mathbf{R}} &= \frac{1}{N}\sum_{\mathbf{k},\mathbf{k}'}\sum_{\mathbf{R}} e^{-i(\mathbf{k}'-\mathbf{k})\cdot\mathbf{R}} e^{-i\mathbf{k}'\cdot\boldsymbol{\delta}_1} d^{\dagger}_{\mathbf{k}'} c_{\mathbf{k}} \\ &= \sum_{\mathbf{k}} e^{-i\mathbf{k}\cdot\boldsymbol{\delta}_1} d^{\dagger}_{\mathbf{k}} c_{\mathbf{k}}, \end{aligned}$$

$$\boxed{\sum_{\mathbf{R}} e^{i(\mathbf{k}'-\mathbf{k})\cdot\mathbf{R}} = N\delta_{\mathbf{k}'\mathbf{k}}.}$$

$$\begin{aligned} \Rightarrow \quad \hat{H} &= t_1 \sum_{\mathbf{k}} \left(e^{-i\mathbf{k}\cdot\boldsymbol{\delta}_1} + e^{-i\mathbf{k}\cdot\boldsymbol{\delta}_2} + e^{-i\mathbf{k}\cdot\boldsymbol{\delta}_3}\right) d^{\dagger}_{\mathbf{k}} c_{\mathbf{k}} \\ &+ t_2 \sum_{\mathbf{k}} \left(e^{-i\mathbf{k}\cdot\mathbf{a}_1} + e^{-i\mathbf{k}\cdot\mathbf{a}_2} + e^{-i\mathbf{k}\cdot\mathbf{a}_3}\right) c^{\dagger}_{\mathbf{k}} c_{\mathbf{k}} \\ &+ t_2 \sum_{\mathbf{k}} \left(e^{-i\mathbf{k}\cdot\mathbf{a}_1} + e^{-i\mathbf{k}\cdot\mathbf{a}_2} + e^{-i\mathbf{k}\cdot\mathbf{a}_3}\right) d^{\dagger}_{\mathbf{k}} d_{\mathbf{k}} + h.c. \\ &+ \Delta \sum_{\mathbf{k}} \left(c^{\dagger}_{\mathbf{k}} c_{\mathbf{k}} - d^{\dagger}_{\mathbf{k}} d_{\mathbf{k}}\right) \\ &= \sum_{\mathbf{k}} \left(c^{\dagger}_{\mathbf{k}}, d^{\dagger}_{\mathbf{k}}\right) \mathsf{H}(\mathbf{k}) \begin{pmatrix} c_{\mathbf{k}} \\ d_{\mathbf{k}} \end{pmatrix}. \end{aligned}$$

$$
\begin{aligned}
\mathsf{H}(\mathbf{k}) &= \begin{pmatrix} 2t_2\sum_i \cos\mathbf{k}\cdot\mathbf{a}_i + \Delta & t_1\sum_i e^{i\mathbf{k}\cdot\boldsymbol{\delta}_i} \\ t_1\sum_i e^{-i\mathbf{k}\cdot\boldsymbol{\delta}_i} & 2t_2\sum_i \cos\mathbf{k}\cdot\mathbf{a}_i - \Delta \end{pmatrix} \\
&= h_0(\mathbf{k}) + \mathbf{h}(\mathbf{k})\cdot\boldsymbol{\sigma},
\end{aligned}
$$

$$
\begin{aligned}
h_0(\mathbf{k}) &= 2t_2\sum_i \cos\mathbf{k}\cdot\mathbf{a}_i, \\
\mathbf{h}(\mathbf{k}) &= \left(t_1\sum_i \cos\mathbf{k}\cdot\boldsymbol{\delta}_i, -t_1\sum_i \sin\mathbf{k}\cdot\boldsymbol{\delta}_i, \Delta\right)
\end{aligned}
$$

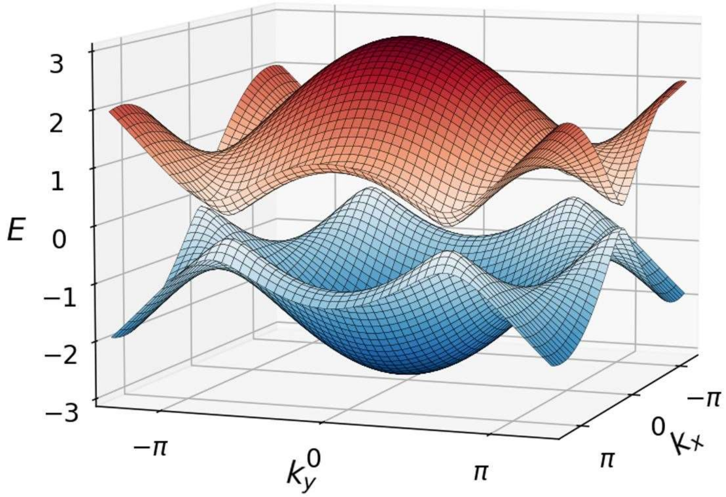

$$\varepsilon_\pm(\mathbf{k}) = h_0(\mathbf{k}) \pm |\mathbf{h}(\mathbf{k})|$$

$$
\begin{aligned}
|\mathbf{h}| &= \sqrt{3t_1^2 + 2t_1^2(\cos\mathbf{k}\cdot\mathbf{a}_1 + \cos\mathbf{k}\cdot\mathbf{a}_2 + \cos\mathbf{k}\cdot\mathbf{a}_3) + \Delta^2} \\
&= \sqrt{3t_1^2 + 2t_1^2 f(\mathbf{k}) + \Delta^2}, \qquad t_1 \simeq 2.7\ eV
\end{aligned}
$$

$$
\begin{aligned}
f(\mathbf{k}) &\equiv \cos\mathbf{k}\cdot\mathbf{a}_1 + \cos\mathbf{k}\cdot\mathbf{a}_2 + \cos\mathbf{k}\cdot\mathbf{a}_3 \\
&= \cos\sqrt{3}ak_x + 2\cos\frac{\sqrt{3}}{2}ak_x \cos\frac{\sqrt{3}}{2}ak_y.
\end{aligned}
$$

Stability of the nodal point in graphene

- TRS $$H(\vec{k})^* = H(-\vec{k})$$
  $$\rightarrow h_x(\vec{k}), h_y(\vec{k}), h_z(\vec{k}) = \text{even, odd, even}$$

- SIS (for graphene, $\pi=\sigma_x$)
  $$\sigma_x H(\vec{k}) \sigma_x = H(-\vec{k})$$
  $$\rightarrow h_x(\vec{k}), h_y(\vec{k}), h_z(\vec{k}) = \text{even, odd, odd}$$

- TRS+SIS $\rightarrow$ no σ_z term ← Co-dimension is 2
  (point degeneracy in 2D BZ)

- Global stability: point degeneracy is further protected by C_3 symmetry (Ch7, Bernevig)

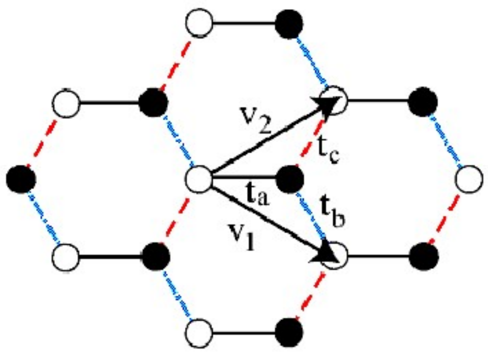

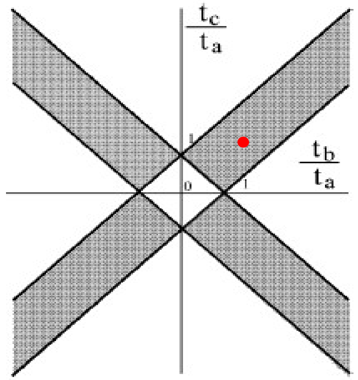

Hasegawa et al, PRB 2006

Low-energy effective Hamiltonian
near Dirac point

$$\mathbf{K}_1 = \frac{2\pi}{a}\left(\frac{2}{3\sqrt{3}}, 0\right),$$
$$\mathbf{K}_2 = \frac{2\pi}{a}\left(\frac{1}{3\sqrt{3}}, \frac{1}{3}\right)$$

Alternative:
$\mathbf{K}_2 = -\mathbf{K}_1$

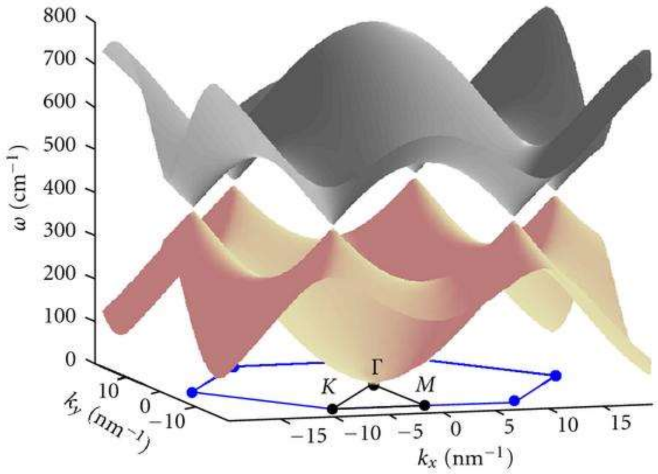

$$\mathbf{k} = \mathbf{K}_i + \mathbf{k}_i, \quad |\mathbf{k}_i| \ll |\mathbf{K}_i|; \; i = 1, 2.$$

$$H_{12}(\mathbf{k}) = t_1\left(e^{i\mathbf{K}_i\cdot\boldsymbol{\delta}_1}e^{i\mathbf{k}_i\cdot\boldsymbol{\delta}_1} + e^{i\mathbf{K}_i\cdot\boldsymbol{\delta}_2}e^{i\mathbf{k}_i\cdot\boldsymbol{\delta}_2} + e^{i\mathbf{K}_i\cdot\boldsymbol{\delta}_3}e^{i\mathbf{k}_i\cdot\boldsymbol{\delta}_3}\right)$$

	$i = 1$	2	3
$\mathbf{K}_1 \cdot \boldsymbol{\delta}_i =$	$+\frac{2\pi}{3}$	$-\frac{2\pi}{3}$	0
$\mathbf{K}_2 \cdot \boldsymbol{\delta}_i =$	$-\frac{2\pi}{3}$	$+\frac{2\pi}{3}$	0
$e^{i\mathbf{K}_{1/2}\cdot\boldsymbol{\delta}_i} =$	$-\frac{1}{2} \mp \frac{\sqrt{3}}{2}i$	$-\frac{1}{2} \pm \frac{\sqrt{3}}{2}i$	1

(rewrite $k_{1,2}$ simply as k)

$$H_{12}(\mathbf{k}) \simeq it_1 a\mathbf{k}\cdot\left(\mp\frac{3}{2}i, -\frac{3}{2}\right)$$
$$= t_1 a\left(\pm\frac{3}{2}k_x - \frac{3}{2}ik_y\right)$$

$$\mathrm{H}(\mathbf{k}) \simeq \begin{pmatrix} \Delta & \frac{3}{2}t_1 a(\pm k_x - ik_y) \\ \frac{3}{2}t_1 a(\pm k_x + ik_y) & -\Delta \end{pmatrix}$$
$$= \hbar v_F(\tau k_x\sigma_x + k_y\sigma_y) + \Delta\sigma_z,$$

valley

$$v_F = \frac{\frac{3}{2}at_1}{\hbar} \simeq \frac{c}{300}$$

Near K_1-valley

$$H = \hbar v_F \vec{\sigma} \cdot (\vec{k} - \vec{K}_1)$$

Under time-reversal, $K_1 \to K_2 = -K_1$

$$H \longrightarrow H' = \hbar v_F \vec{\sigma}^* \cdot \left(-\vec{k} - \vec{K}_1\right) = -\hbar v_F \vec{\sigma}^* \cdot \left(\vec{k} + \vec{K}_1\right)$$

As a result, the Berry curvature and orbital magnetization at K_1 and $-K_1$ are opposite in signs

- Effective Hamiltonian near degenerate point

$$H_0 = \hbar v_F(\pm k_x\sigma_x + k_y\sigma_y) + \Delta\sigma_z \text{ at } \pm K, \qquad \hbar v_F \equiv \frac{3}{2}t_1 a$$

- Berry curvature

$$F_{z\tau}^{\pm}(\mathbf{k}) = \mp\tau\frac{1}{2}\frac{\hbar^2 v_F^2\Delta}{h^3}$$

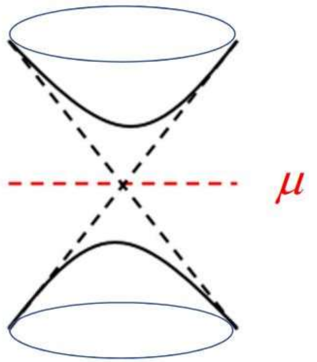

$$\int_{all} d^2k\, F_\tau^{\pm} = \mp\tau\pi$$ (Drop sub z)

➡ $$\sigma_H = \frac{e^2}{h}\frac{1}{2\pi}\int d^2k F_\tau^- = \frac{\tau}{2}\frac{e^2}{h}$$

Total Hall conductivity is zero due to the cancellation between 2 valleys.

- Gapless limit (at +***K***):

➡ Berry phase (surrounding +***K***): $\gamma_C = \mp\pi$

Berry phase remains the same

➡ $$F^{\pm}(\vec{k}) = \mp\pi\delta^2(\vec{k})$$

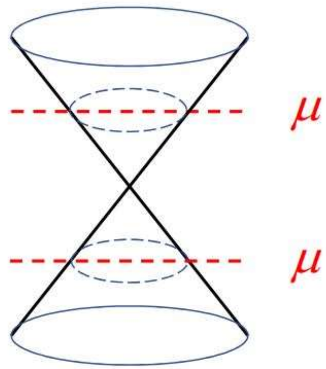

Graphene in magnetic field

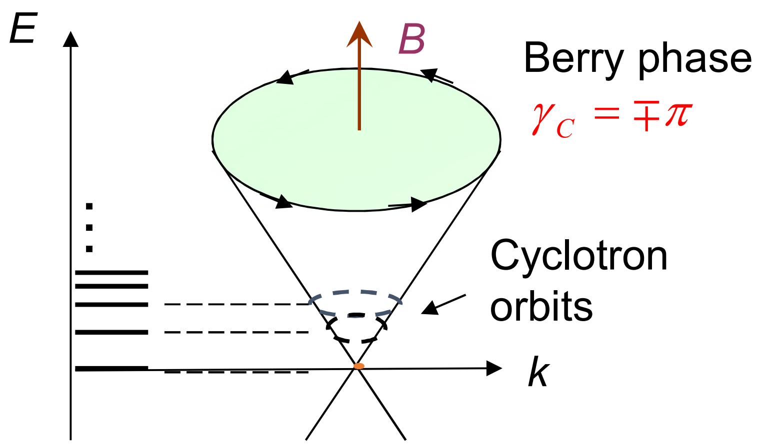

Bohr-Sommerfeld quantization
(Kittel)

$$\underbrace{\frac{1}{2}\oint_C \left(\vec{k} \times d\vec{k}\right) \cdot \hat{z}}_{\text{Orbital area}} = 2\pi\left(n + \frac{1}{2} - \frac{\gamma_C}{2\pi}\right)\frac{eB}{\hbar}$$

Correction from Berry phase

$$\pi k^2 = 2\pi\left(n + \cancel{\frac{1}{2}} - \cancel{\frac{\gamma_C}{2\pi}}\right)\frac{eB}{\hbar}$$

$$E(k) = \hbar v_F k$$

$$E_n = v_F\sqrt{2eB\hbar n}$$ Landau levels

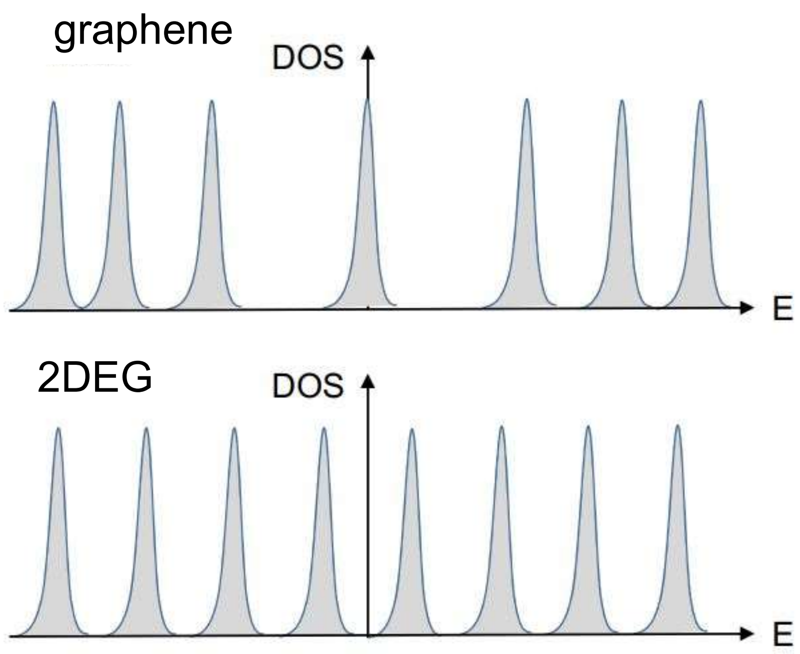

STM experiment
(Cheng et al, PRL 2010)

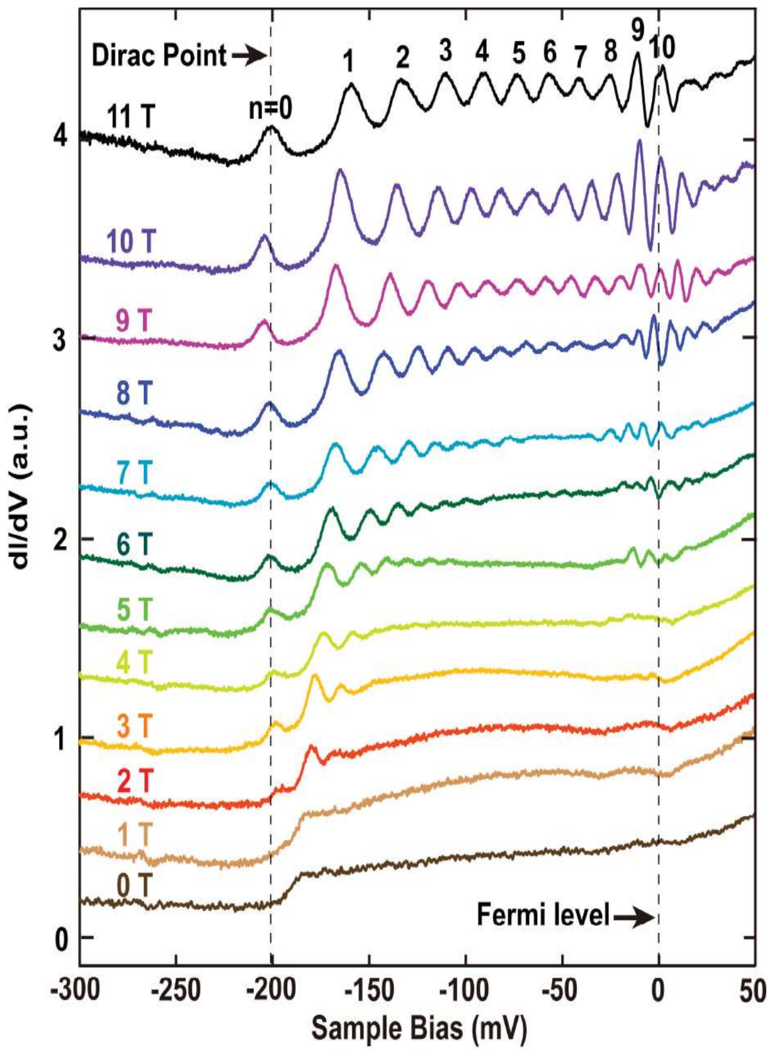

Quantum Hall effect in graphene

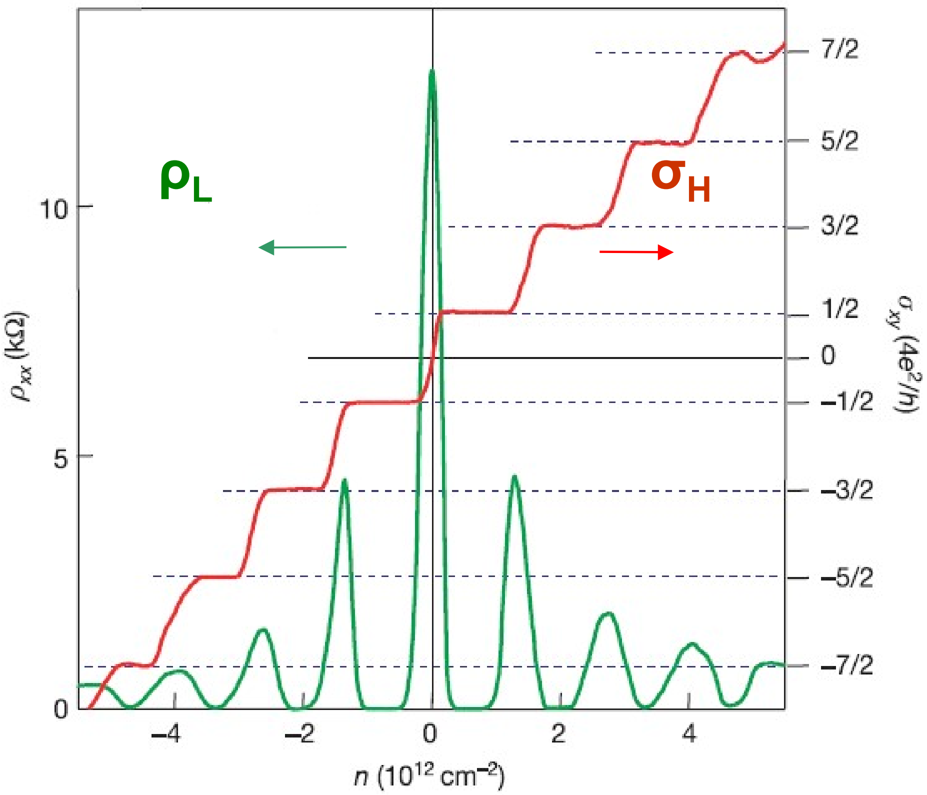

Novoselov et al, Nature 2005

Valley Hall effect (Xiao et al, PRL 2007)

B = 0

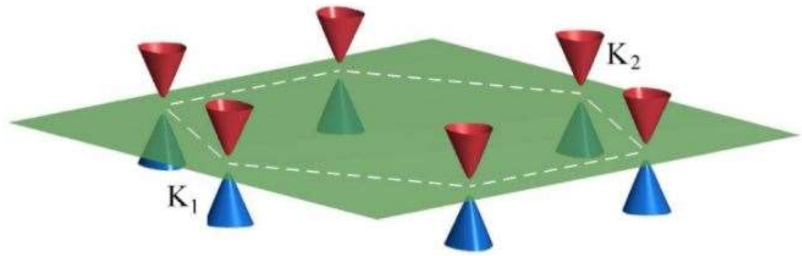

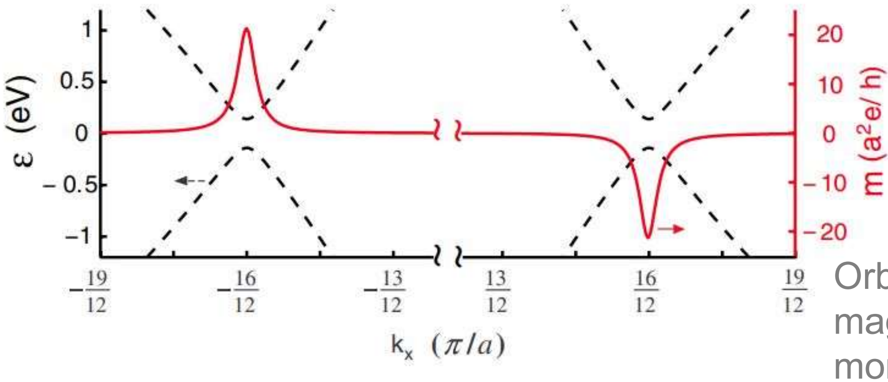

$\sim \Omega$

Orbital magnetic moment

Opposite anomalous velocities

from two valleys

$$\mathbf{v}_n(\mathbf{k}) = \frac{1}{\hbar}\frac{\partial \varepsilon_{n\mathbf{k}}}{\partial \mathbf{k}} + \boxed{\frac{e}{\hbar}\mathbf{E}\times\mathbf{F}_n(\mathbf{k})}$$

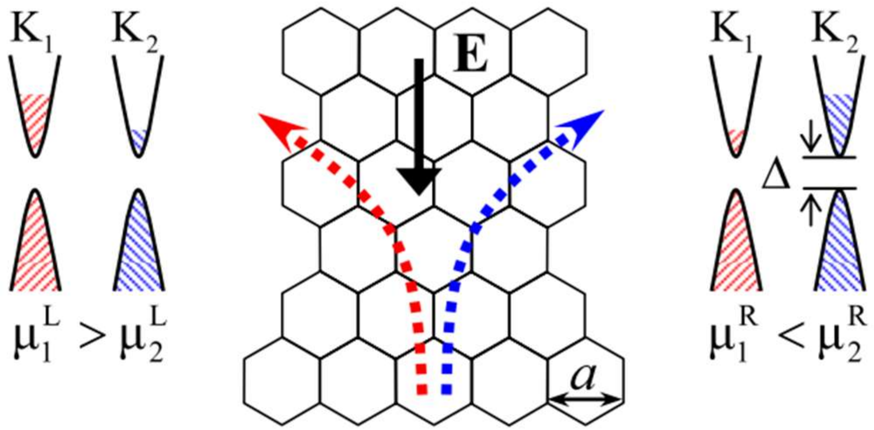

VALLEYTRONICS

Detecting topological currents in graphene superlattices

Science, 2014

R. V. Gorbachev,[1,2*] J. C. W. Song,[3,4*] G. L. Yu,[1] A. V. Kretinin,[2] F. Withers,[2] Y. Cao,[1] A. Mishchenko,[1] I. V. Grigorieva,[2] K. S. Novoselov,[2] L. S. Levitov,[3*] A. K. Geim[1,2]†

Graphene on hBN (breaking inversion symm → 2Δ = 30 meV)

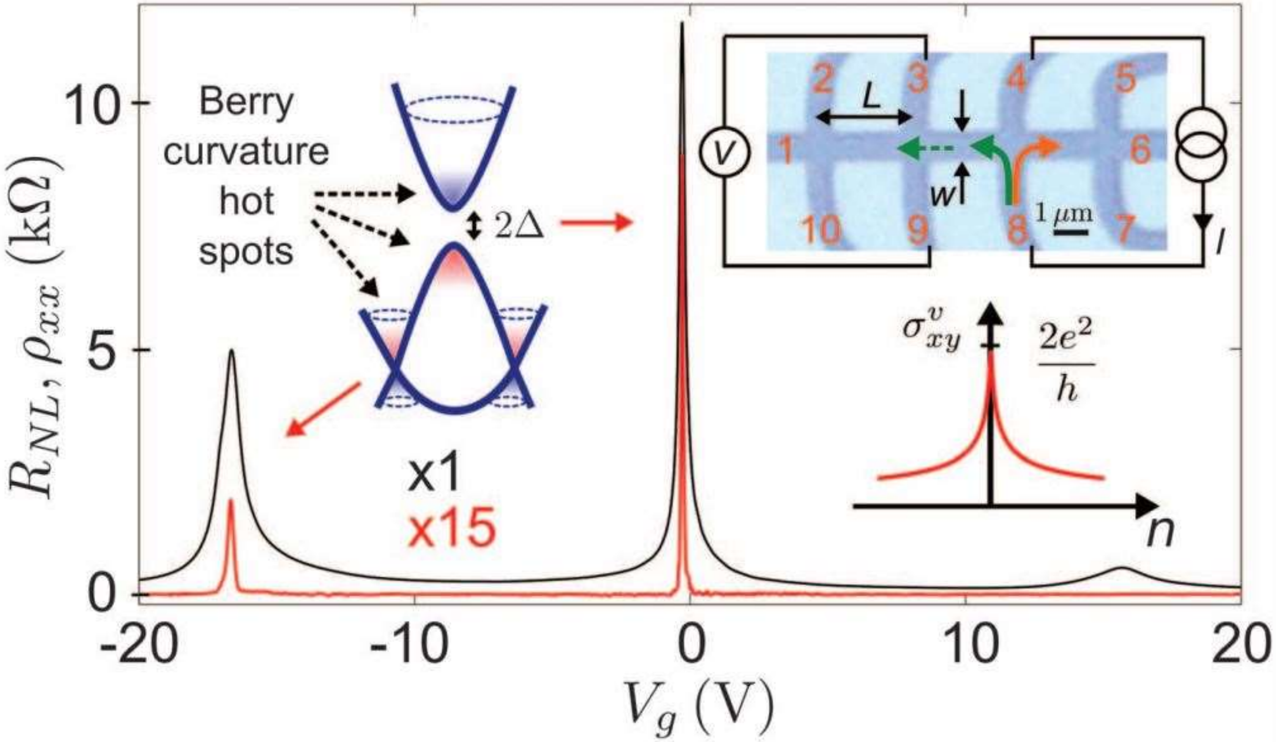

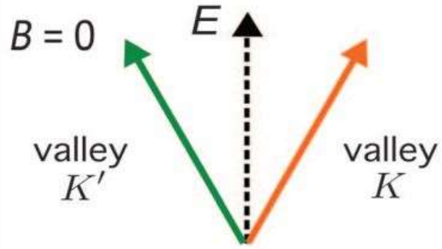

2D material: graphene, silicene, hBN, TMD …e6c

Graphene (with SIS)

monolayer MoS_2 (without SIS)

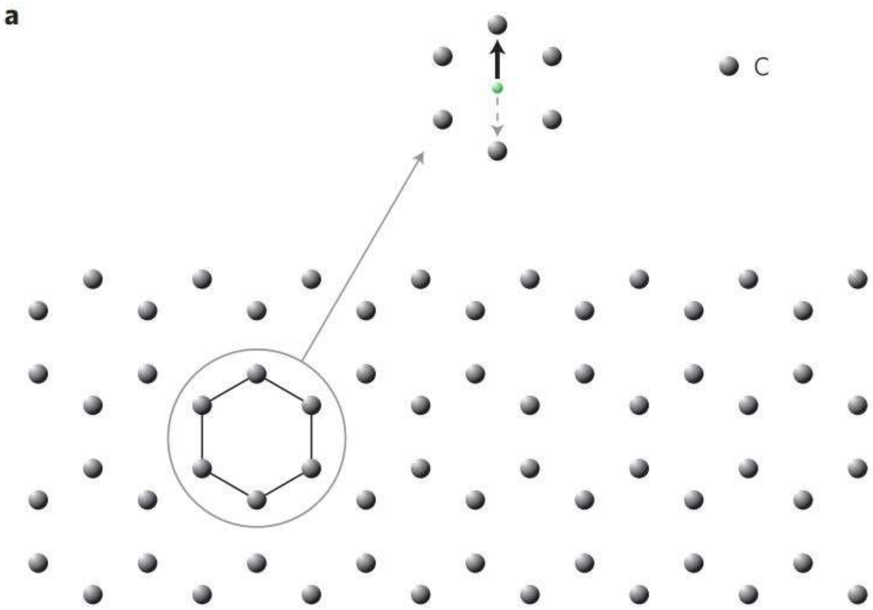

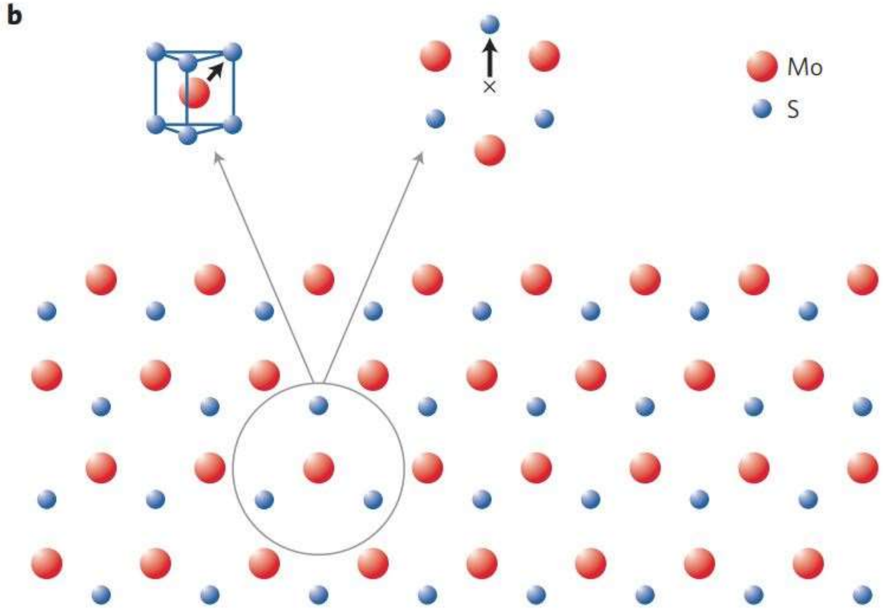

Graphene on hBN breaks SIS,
opens a gap ~ 30 mV

An energy gap ~ 1.9 eV
(easier for optical and electrical control)

2 Transition Metal Dichalcogenide (TMD)

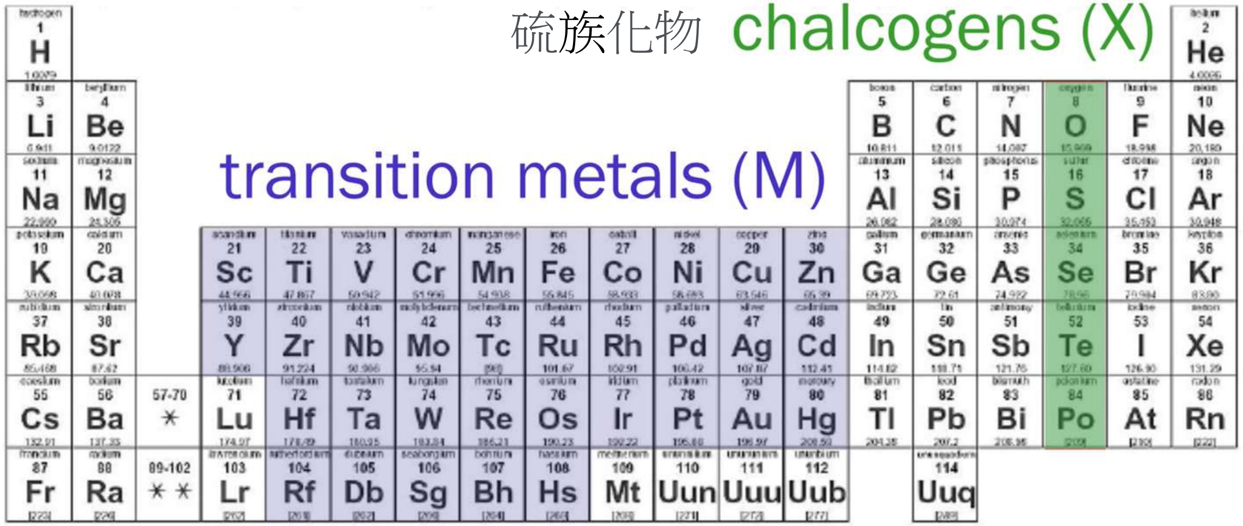

MX_2 stable as a monolayer

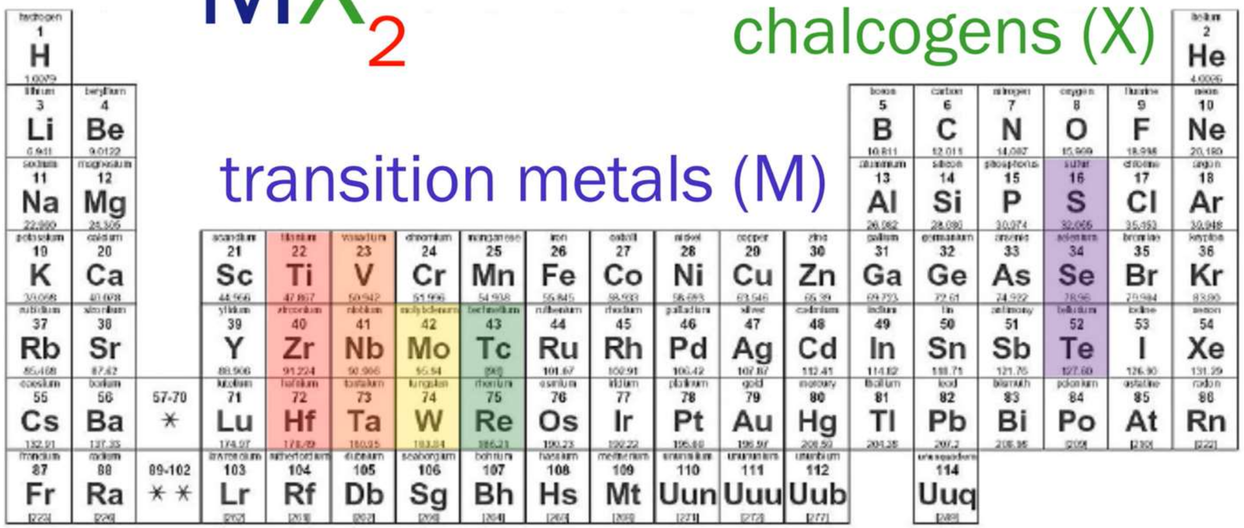

3 possible forms of MX_2:

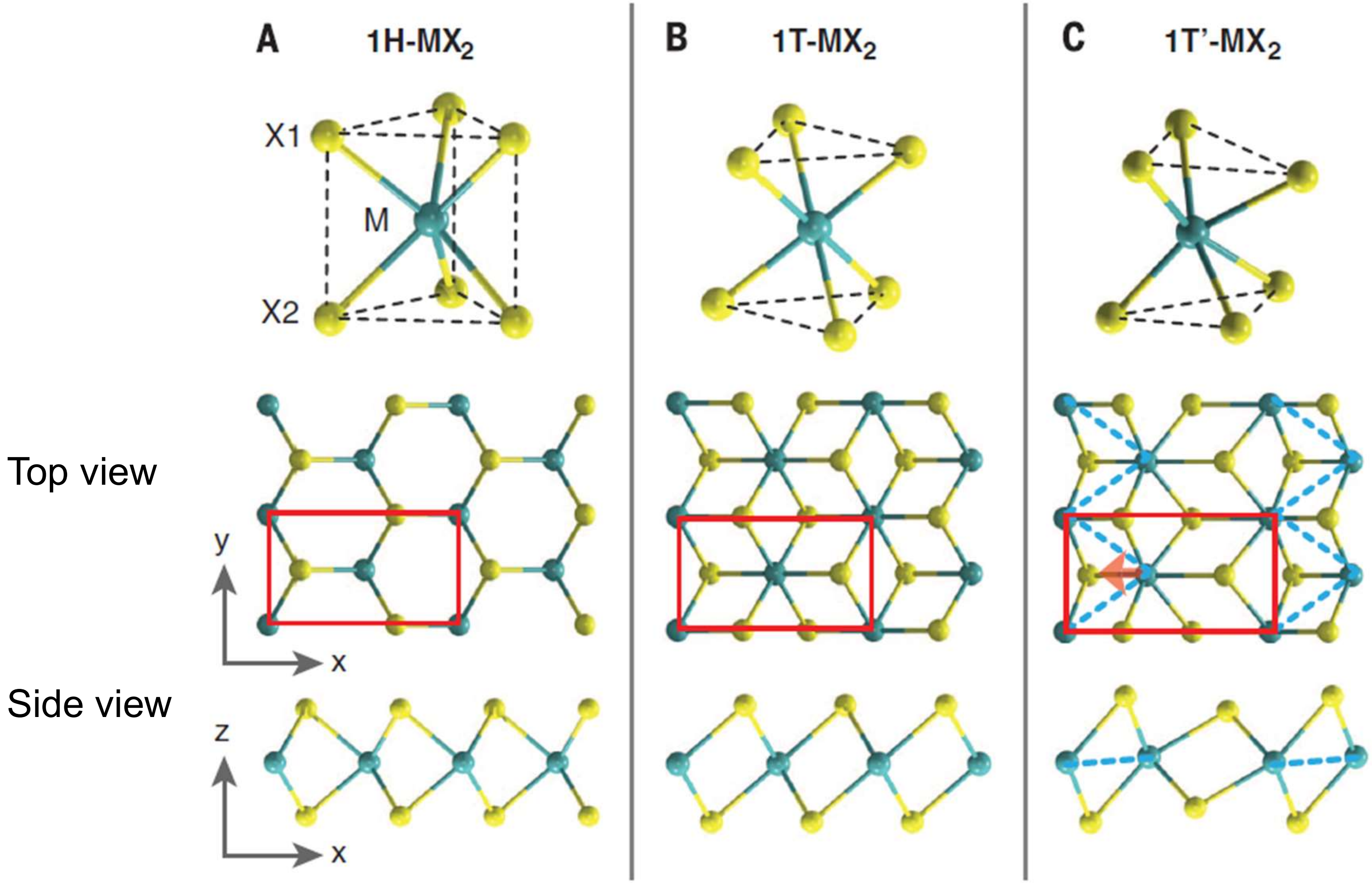

Fig from Qian et al, Science 2014

Transition Metal Dichalcogenide: MoS_2

- Bulk indirect band gap (with SIS); single layer direct band gap (without SIS)
- Massive Dirac fermion
- Large SO coupling, spin-valley locking (due to Kramer degeneracy)
- Room temperature mobility 3-4 order of magnitude lower than in graphene
- Strong Coulomb interaction, excitons

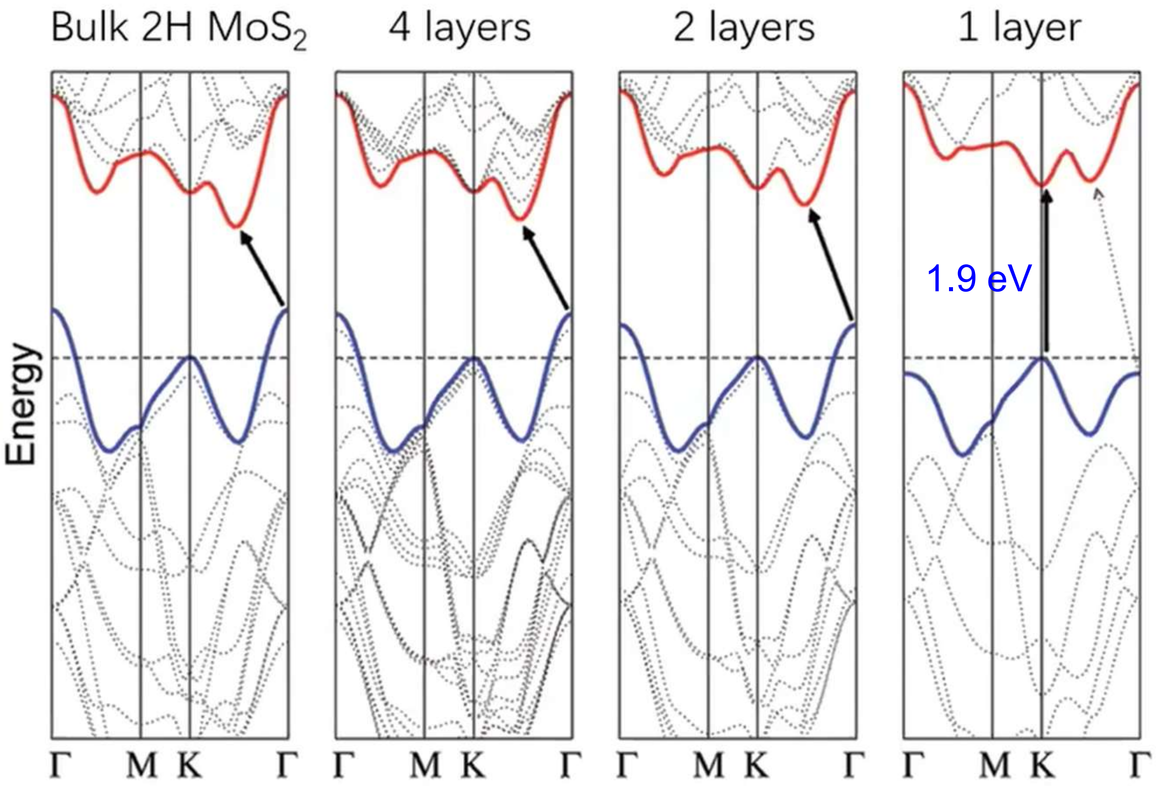

Splendiani et al, Nano Lett 2010

1 layer

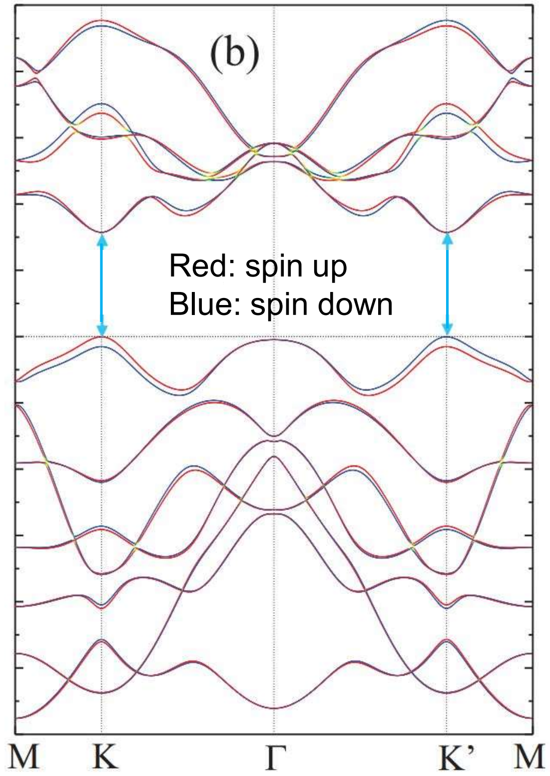

Feng et al, PRB 2012

Massive Dirac points of MoS_2 monolayer

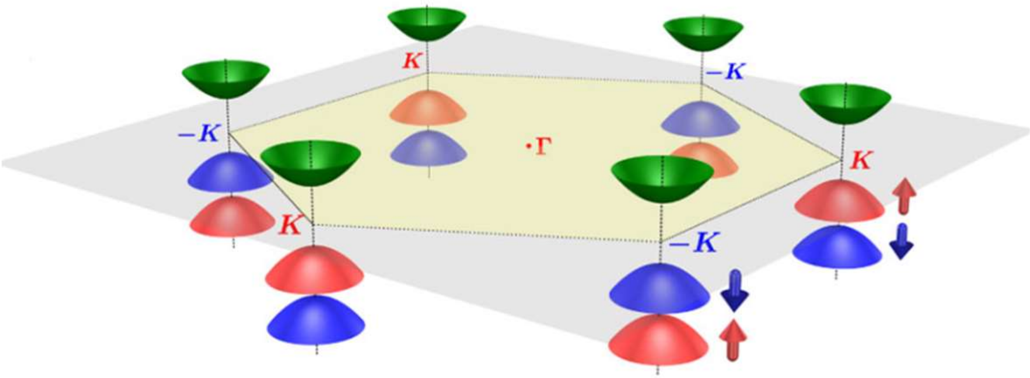

Fig from Xiao et al, PRL 2012

Effective 2-band model near Dirac points

$$H = \alpha(\tau k_x \sigma_x + k_y \sigma_y) + \Delta' \sigma_z + \frac{\lambda}{2}$$

$$\Delta' \equiv \Delta - \lambda/2$$

$$\varepsilon_k^{c/v} = \pm\sqrt{\alpha^2 k^2 + \Delta'^2} + \frac{\lambda}{2}$$

Berry curvature

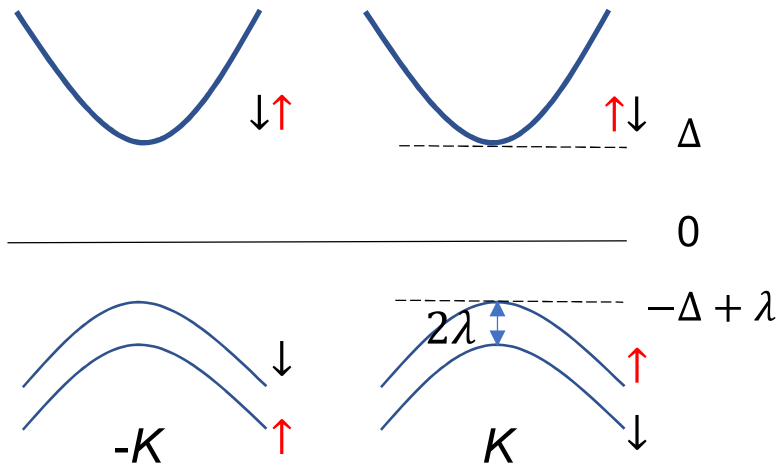

$$F_c^\tau(\mathbf{k}) = \frac{\tau}{2} \frac{\alpha^2 \Delta'}{\left[\alpha^2 k^2 + \Delta'^2\right]^{3/2}}$$

Opposite valleys have opposite BCs

For partially-filled valence band,

$$\begin{aligned} \sigma_H^\tau &= \frac{1}{2\pi} \int d^2k F_c^\tau(\mathbf{k}) \\ &= \frac{\tau}{2}\left[1 - \frac{\Delta'}{\sqrt{\alpha^2 k_F^2 + \Delta'^2}}\right] \end{aligned}$$

The Berry curvatures of monolayer MoS_2

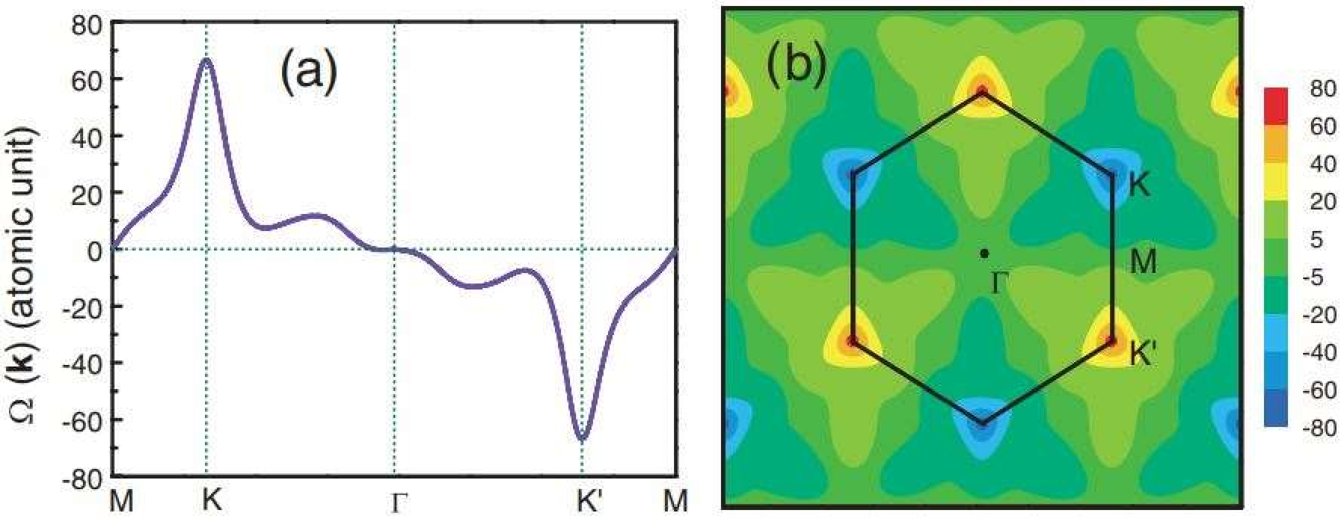

Feng et al, PRB 2012

VALLEYTRONICS Science, 2014

The valley Hall effect in MoS_2 transistors

K. F. Mak,[1,2]* K. L. McGill,[2] J. Park,[1,3] P. L. McEuen[1,2]*

Lee et al, Nature Nano Tech, 2016

Bilayer MoS_2 with SIS (broken by E field)

Local Kerr signal

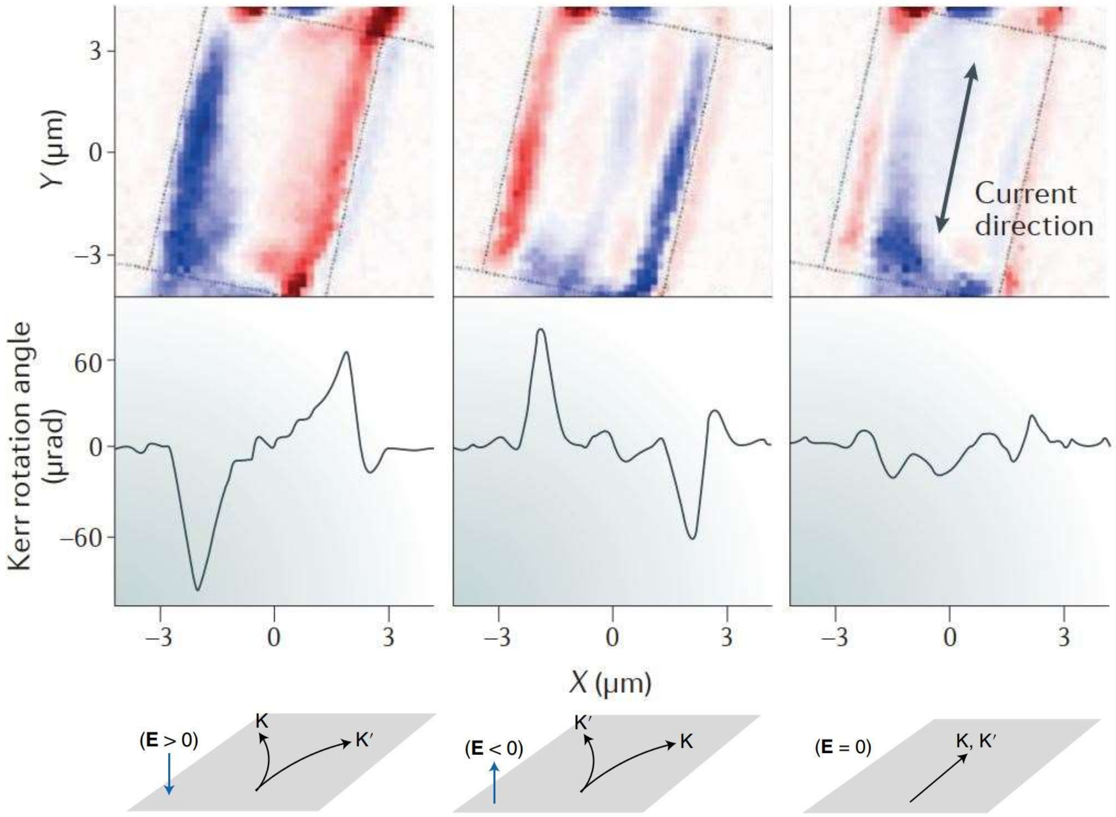

Valley-selective optical pumping
(Yao et al, PRB 2008)

- *K*, *K*' population imbalance induced by optical pumping

→ photo-induced AHE

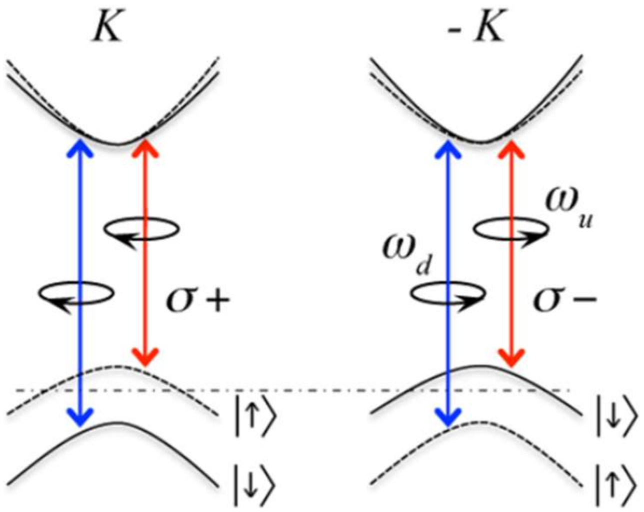

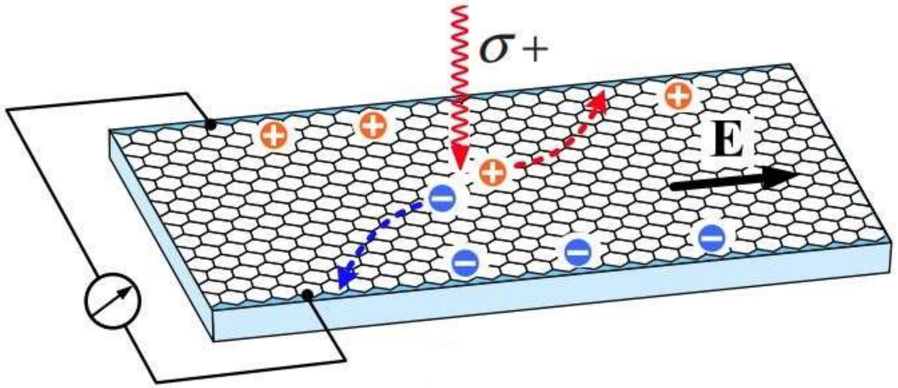

Optical field couples only to the orbital part of the wave function and spin is conserved in the optical transitions.

Solid circles: electrons - and holes + in K-valley. The currents add up.

Xiao et al, PRL 2012

Two-dimensional material

1 • Graphene
  - symmetries
  - Effective Hamiltonian

2 • Transition metal dichalcogenide
  - Berry curvature
  - Optical transitions

3 • Haldane model
  - Haldane flux
  - Berry curvature

4 • Twisted bilayer graphene

First, electron hopping in a magnetic field

- Aharonov-Bohm (AB) phase

For a closed loop C,

$$\psi' = e^{i\frac{e}{\hbar}\oint_C d\vec{r}\cdot\vec{A}}\psi = e^{2\pi i\frac{\Phi_B}{\Phi_0}},\ \Phi_0 \equiv h/e$$

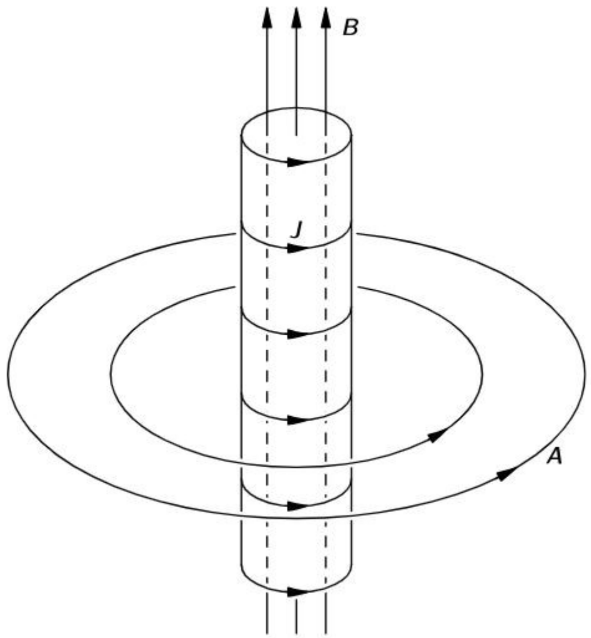

- AB phase and electron hopping

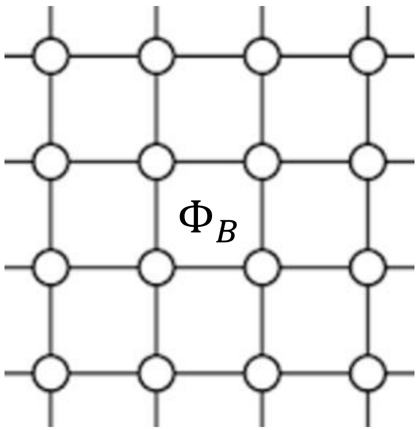

3 Haldane's graphene model, PRL 1989

(no net magnetic field, but TRS is broken)

$$H = -t_1 \sum_{<i,j>} c_i^+ c_j + \Delta \sum_i \xi_i c_i^+ c_i + \boxed{t_2 \sum_{<<i,j>>} e^{i\nu_{ij}\phi} c_i^+ c_j} \quad \text{NNN}$$

^ break SIS ^ break TRS

As a result of Haldane flux

$$\begin{aligned}
\mathbf{R}_A &\rightarrow \mathbf{R}_A + \mathbf{a}_i \text{ get } e^{-i\phi}, \; i = 1,2,3 \\
\mathbf{R}_A &\rightarrow \mathbf{R}_A - \mathbf{a}_i \text{ get } e^{+i\phi}, \\
\mathbf{R}_B &\rightarrow \mathbf{R}_A + \mathbf{a}_i \text{ get } e^{+i\phi}, \\
\mathbf{R}_B &\rightarrow \mathbf{R}_A - \mathbf{a}_i \text{ get } e^{-i\phi}.
\end{aligned}$$

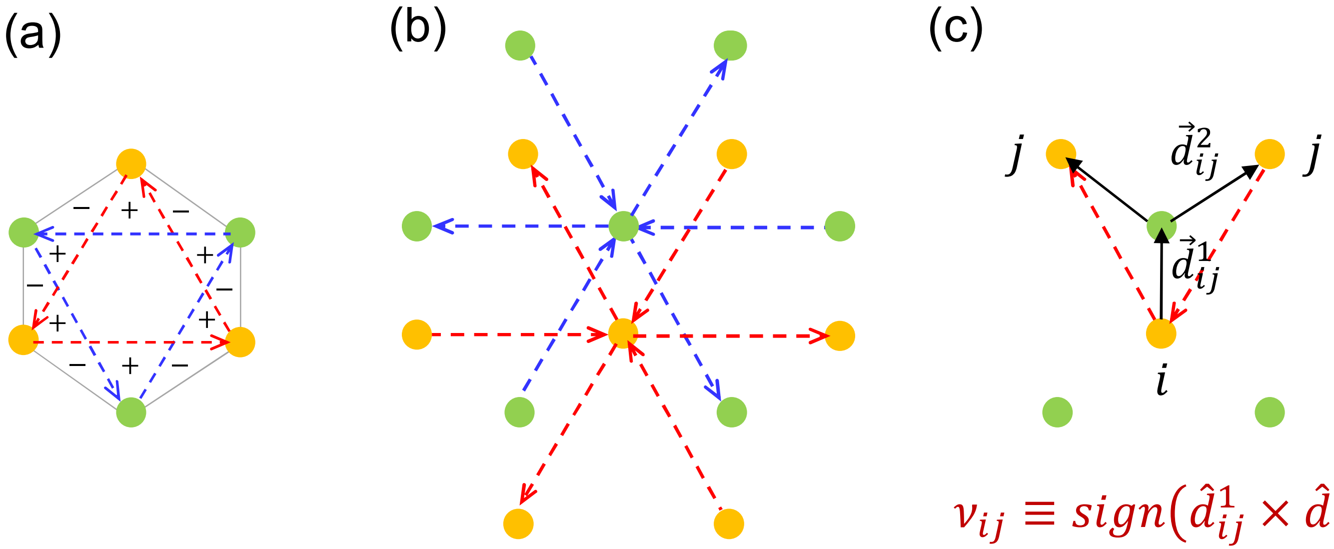

$$\nu_{ij} \equiv sign\left(\hat{d}_{ij}^1 \times \hat{d}_{ij}^2\right)_z$$

NNN coupling

$$
\begin{aligned}
\hat{H}_{NNN} &= t_2 \sum_{\mathbf{R}} \sum_{i=1}^{3} \left(c^{\dagger}_{\mathbf{R}+\mathbf{a}_i} c_{\mathbf{R}} e^{-i\phi} + h.c. \right) \\
&+ t_2 \sum_{\mathbf{R}} \sum_{i=1}^{3} \left({}^{\dagger}_{\mathbf{R}+\mathbf{a}_i} d_{\mathbf{R}} e^{+i\phi} + h.c. \right) . \\
&= 2t_2 \sum_{\mathbf{k}} \sum_{i} \left[\cos(\mathbf{k}\cdot\mathbf{a}_i + \phi) c^{\dagger}_{\mathbf{k}} c_{\mathbf{k}} + \cos(\mathbf{k}\cdot\mathbf{a}_i - \phi) d^{\dagger}_{\mathbf{k}} d_{\mathbf{k}} \right] \\
&= \sum_{\mathbf{k}} \left(c^{\dagger}_{\mathbf{k}}, d^{\dagger}_{\mathbf{k}} \right) \mathsf{H}_{NNN}(\mathbf{k}) \begin{pmatrix} c_{\mathbf{k}} \\ d_{\mathbf{k}} \end{pmatrix}
\end{aligned}
$$

$$
\boxed{\mathsf{H}_{NNN}(\mathbf{k}) = 2t_2 \begin{pmatrix} \sum_i \cos(\mathbf{k}\cdot\mathbf{a}_i + \phi) & 0 \\ 0 & \sum_i \cos(\mathbf{k}\cdot\mathbf{a}_i - \phi) \end{pmatrix}}
$$

$$
\Rightarrow \quad \mathsf{H}(\mathbf{k}) = \frac{h_{11} + h_{22}}{2} + \mathbf{h}\cdot\boldsymbol{\sigma}
$$

$$
\mathbf{h} = \left(t_1 \sum_i \cos\mathbf{k}\cdot\boldsymbol{\delta}_i, -t_1 \sum_i \sin\mathbf{k}\cdot\boldsymbol{\delta}_i, \boxed{\frac{h_{11} - h_{22}}{2}} + \Delta \right)
$$

$$
= \underline{-2t_2 \sum_i \sin\mathbf{k}\cdot\mathbf{a}_i \sin\phi + \Delta}
$$

Near Dirac point

$$h_3(\mathbf{k}) = \pm 3\sqrt{3} t_2 \sin\phi + \Delta + O(k^2).$$

let $h_3 = m_\tau(\phi, \Delta)$ a ϕ-dependent effective mass

$$\mathrm{H}_\tau(\mathbf{k}) = \frac{h_{11} + h_{22}}{2} + \begin{pmatrix} m_\tau & \hbar v_F(\tau k_x - i k_y) \\ \hbar v_F(\tau k_x + i k_y) & -m_\tau \end{pmatrix}$$

$$F^{+}_{z\tau}(\mathbf{k}) = \frac{\tau}{2} \frac{\hbar^2 v_F^2 m_\tau}{(\hbar^2 v_F^2 k^2 + m_\tau^2)^{3/2}}$$

The Dirac gap is closed when

$$\boxed{m_\pm(\phi, \Delta) = \pm 3\sqrt{3} t_2 \sin\phi + \Delta = 0}$$

Fig from Atteia's thesis, 2018

Phase diagram Zero-field quantum Hall effect phases ($\nu = \pm 1$, where $\sigma^{xy} = \nu e^2/h$) occur if $|M/t_2| < 3\sqrt{3}|\sin\phi|$.

(a)

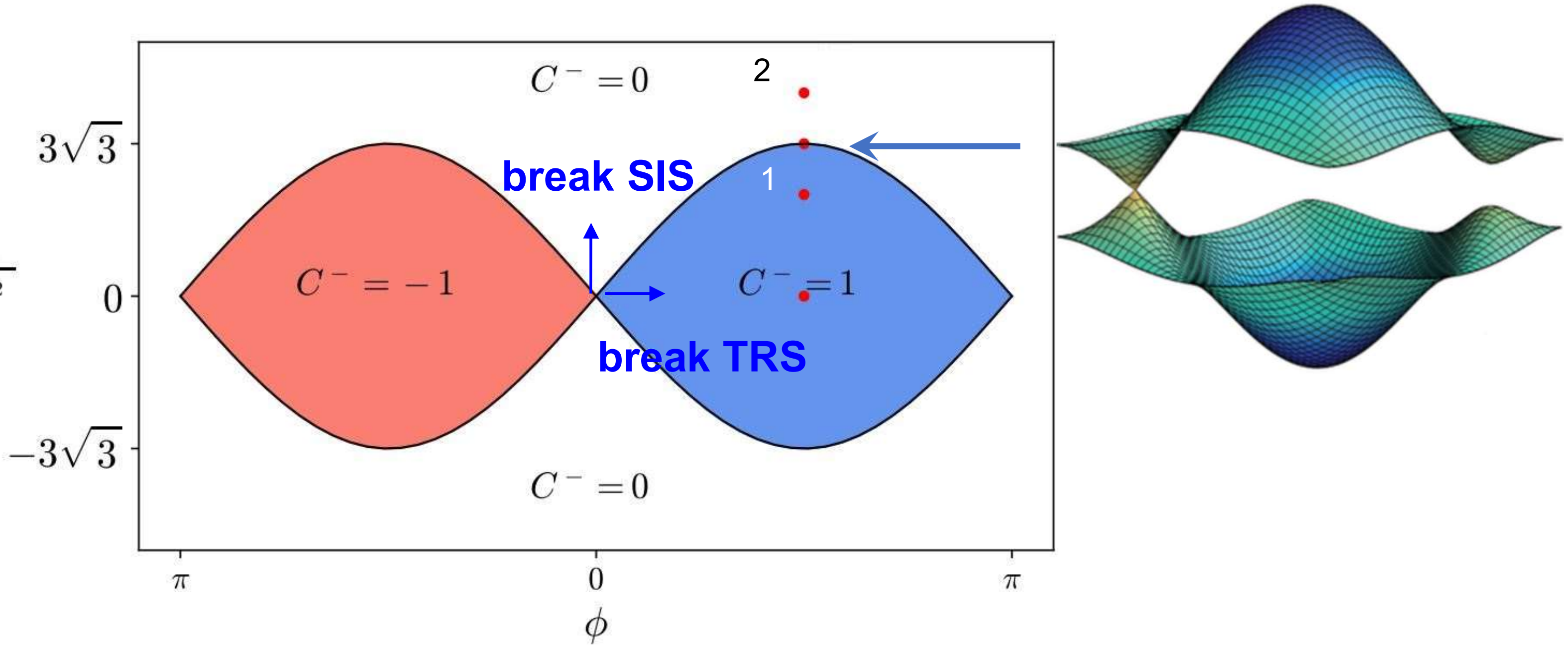

(b) Berry curvatures of point 1 (left) and 2 (right)

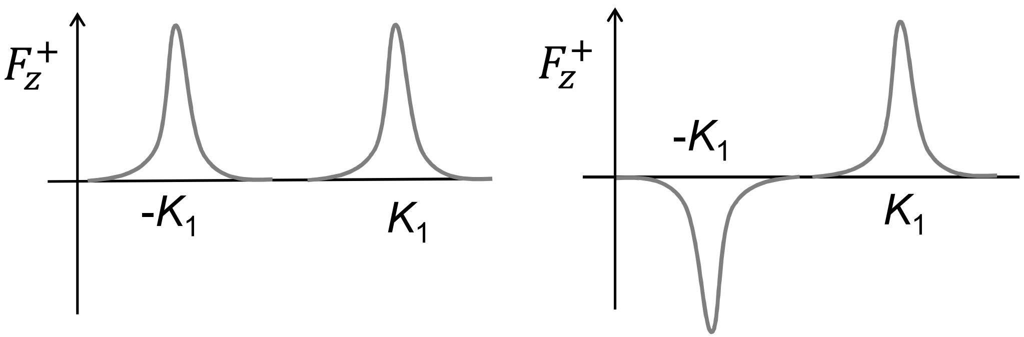

3' Kane-Mele model = 2 copies of Haldane model

(Kane and Mele, PRL 2005)

The first example of topological insulator

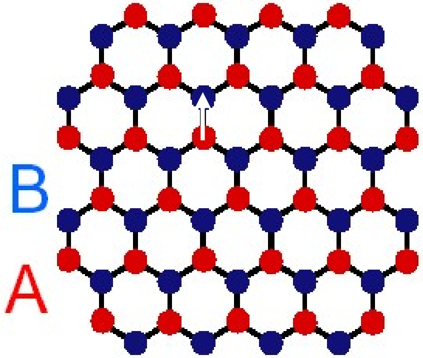

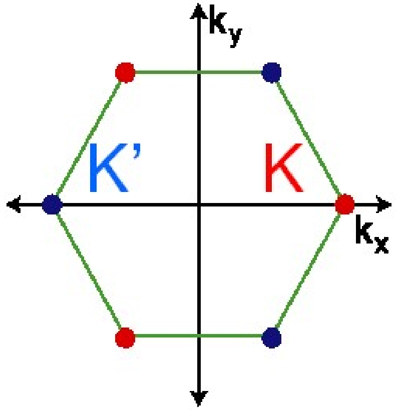

$$H = -t \sum_{<i,j>} c_i^+ c_j$$

$$c_i = \begin{pmatrix} a_{i\uparrow} \\ a_{i\downarrow} \\ b_{i\uparrow} \\ b_{i\downarrow} \end{pmatrix}$$

Sublattice potential $\quad +\lambda_{sub} \sum_i \xi_i c_i^+ c_i$

Intrinsic SO coupling $\quad + i\lambda_{SO} \sum_{<<i,j>>} \nu_{ij} c_i^+ s_z c_j$

Graphene:

$\sim \; L_z S_z \sim 10^{-3} meV$

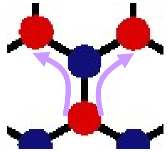

- All of the terms respect TR symm
- H_{sub} breaks space inversion symm
- H_{so} does not break TRS or SIS

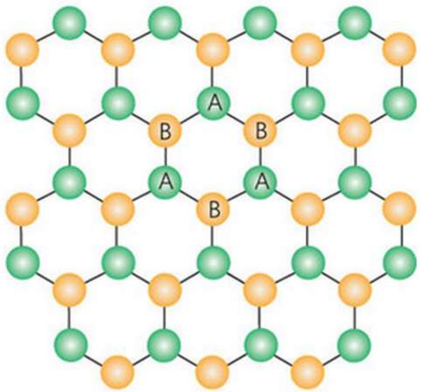

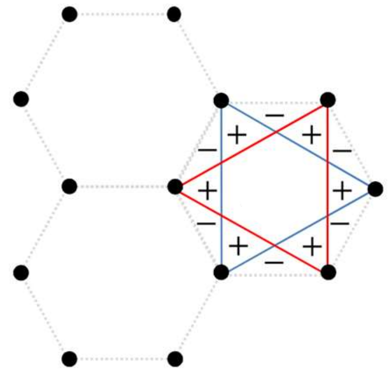

- **Semenoff mass** (PRL 1984)
- **Haldane mass** (PRL 1989)
- **Kane-Mele mass** (PRL 2005)

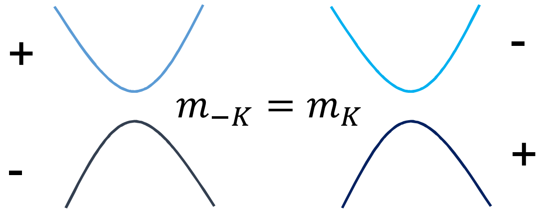

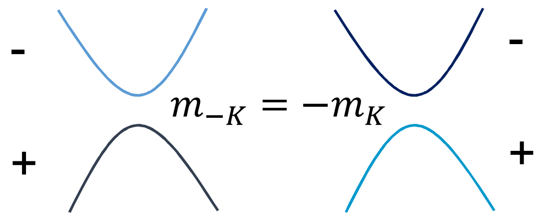

~ 2 copies of
Haldane model

$$H^{\pm K} = H_0 + m\sigma_z$$

$$H^{\pm K} = H_0 \pm m\sigma_z$$

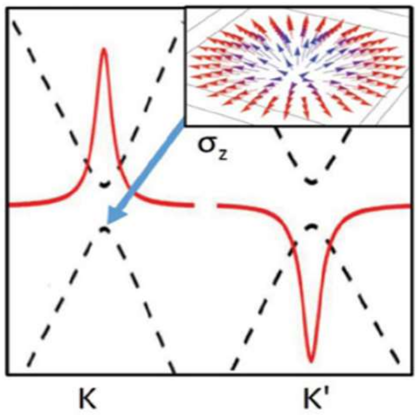

$\sigma_H = 0$

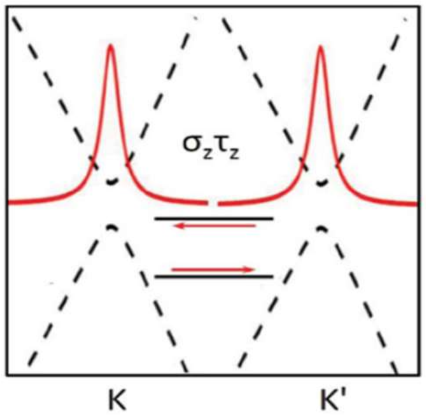

$\sigma_H = e^2/h$ (QAHE)

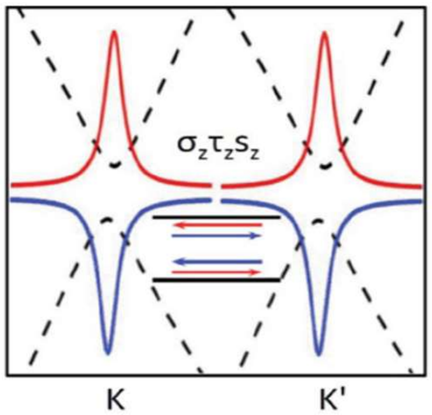

QSHE

Fig from Ren et al, Rep Prog Physics 2015

Graphene with edge (no topology)

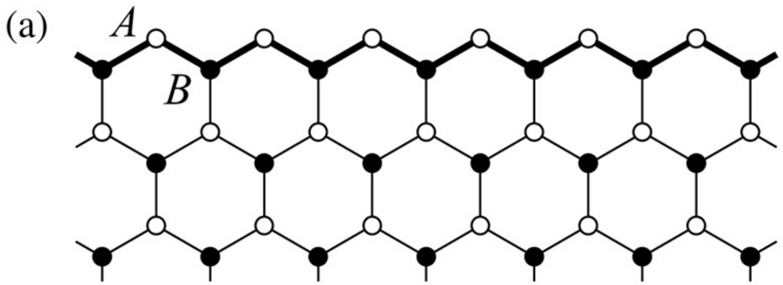

Zigzag edge

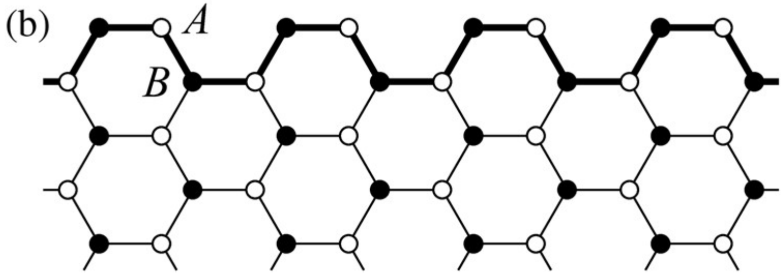

Armchair edge

Edge states for zigzag edge (Fujita, 1996)

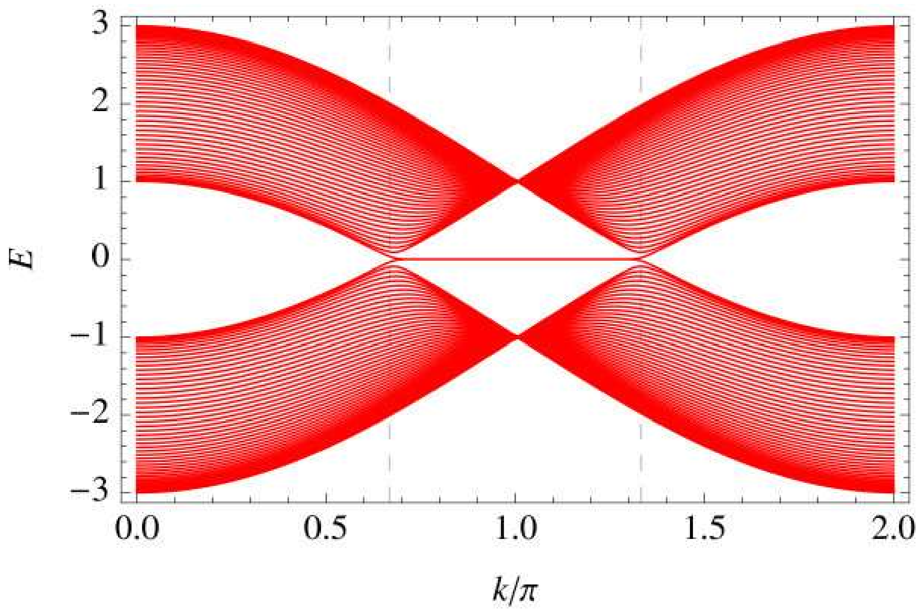

Edge state in different graphene models (for zigzag edge)

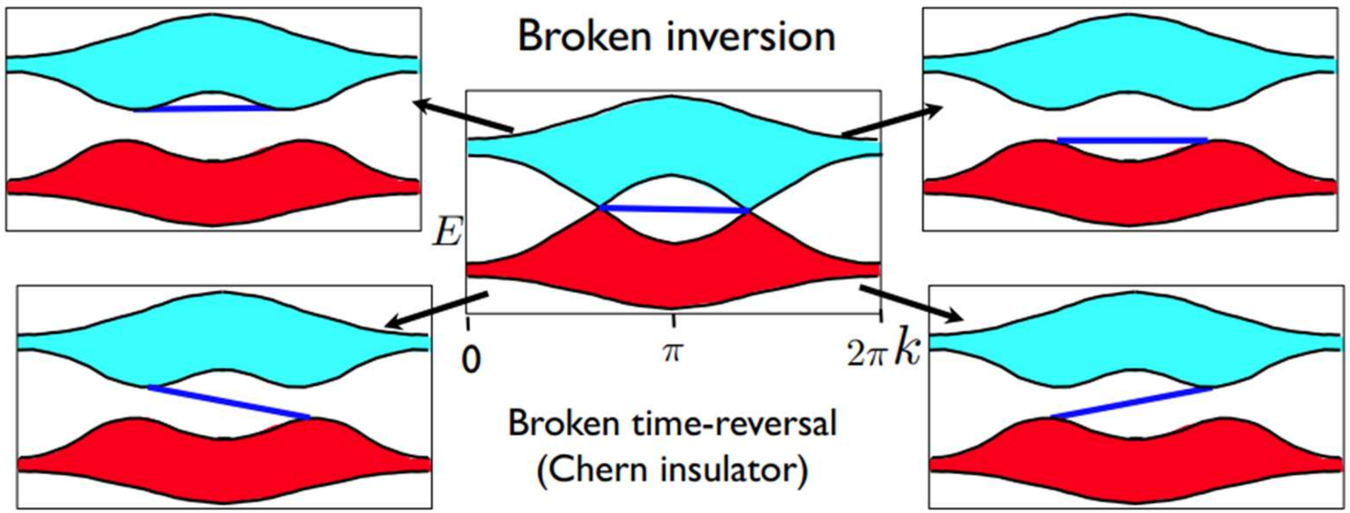

Haldane, Nobel lecture

Kane-Mele model

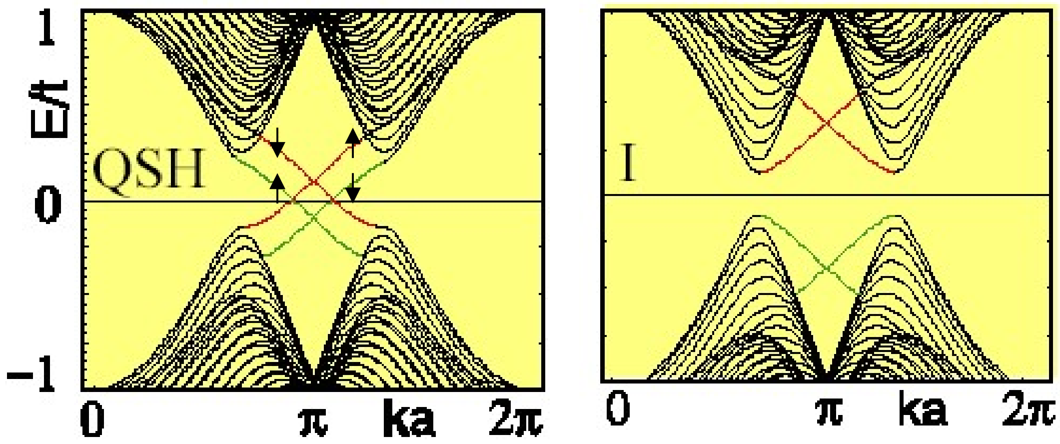

Bilayer graphene

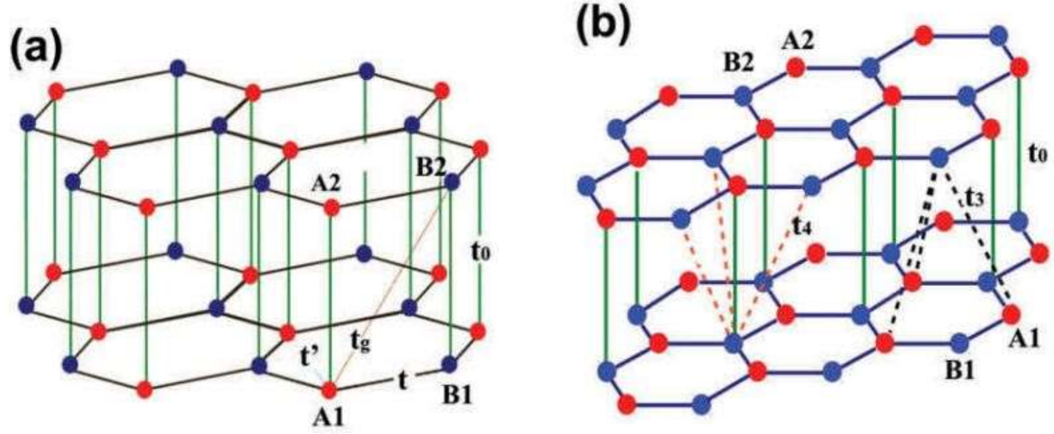

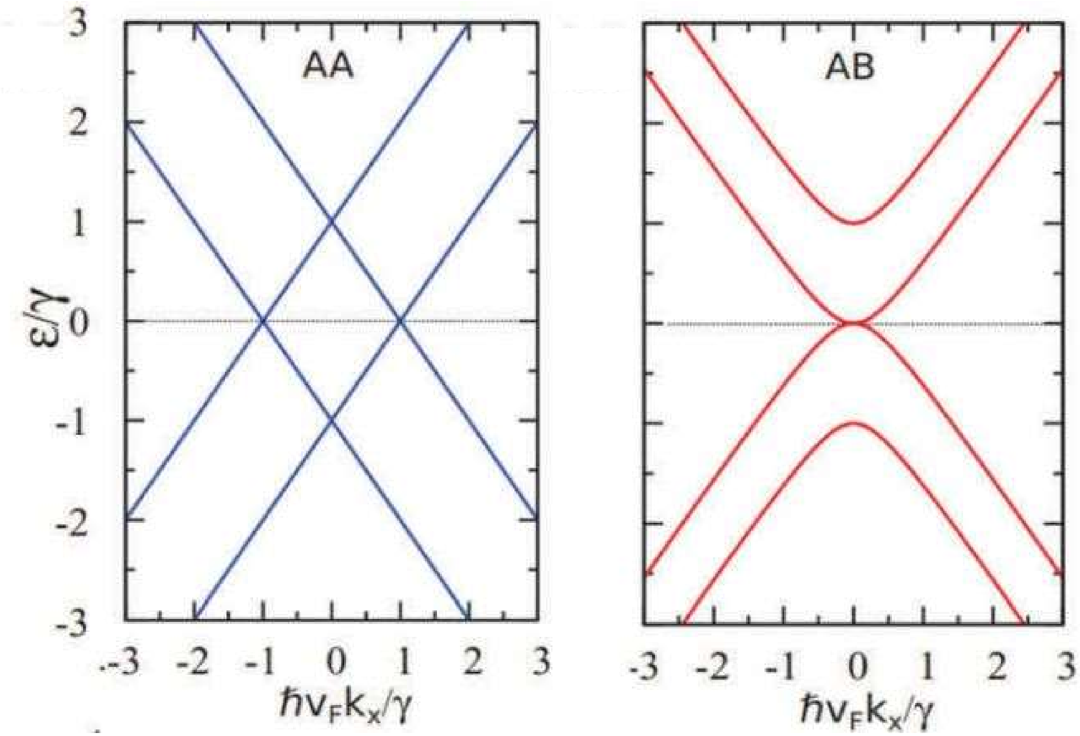

Trilayer graphene

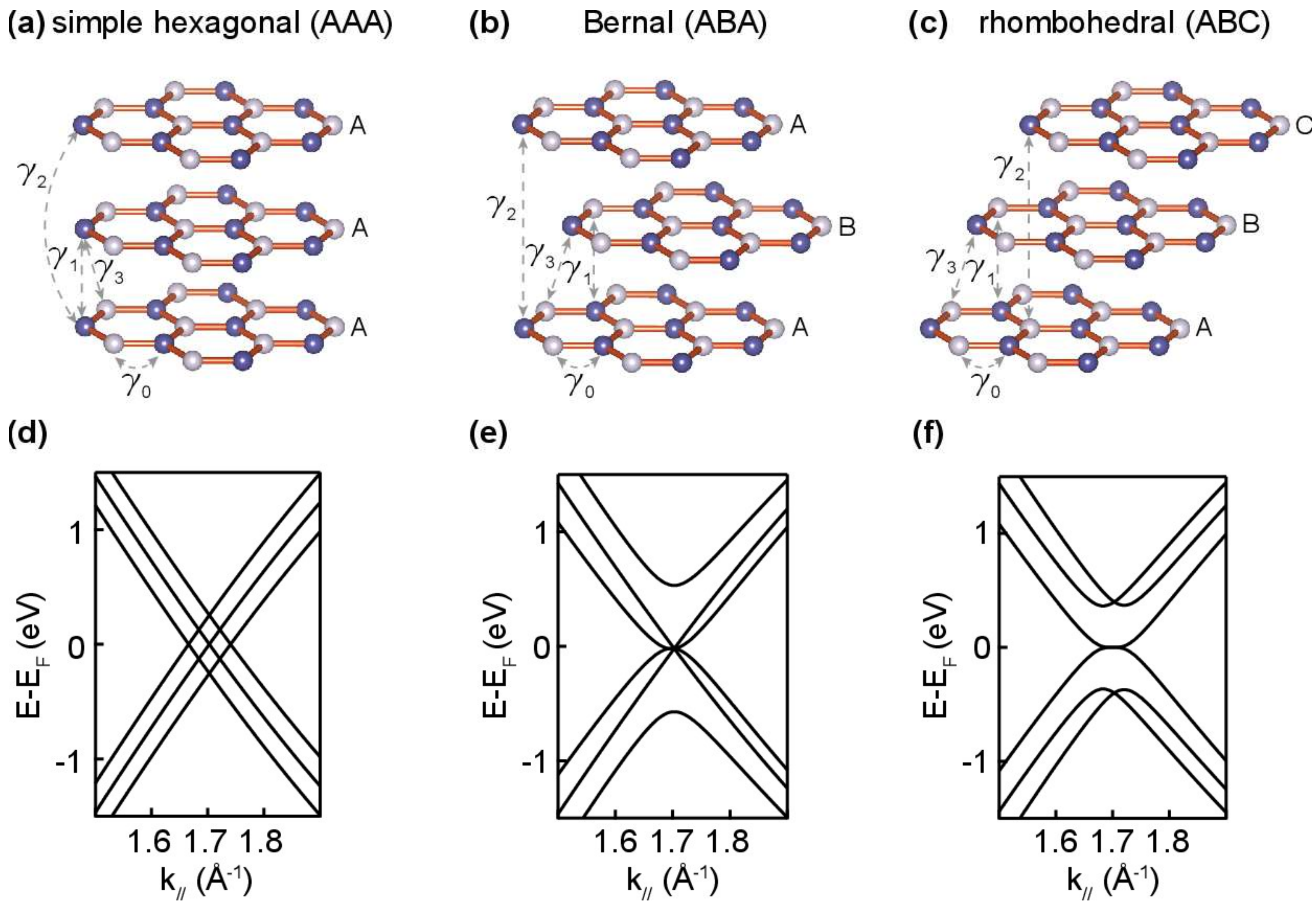

Bao et al, Nano Lett 2017

4 Twisted bi-layer graphene (TBLG) Santos et al, PRL 2007

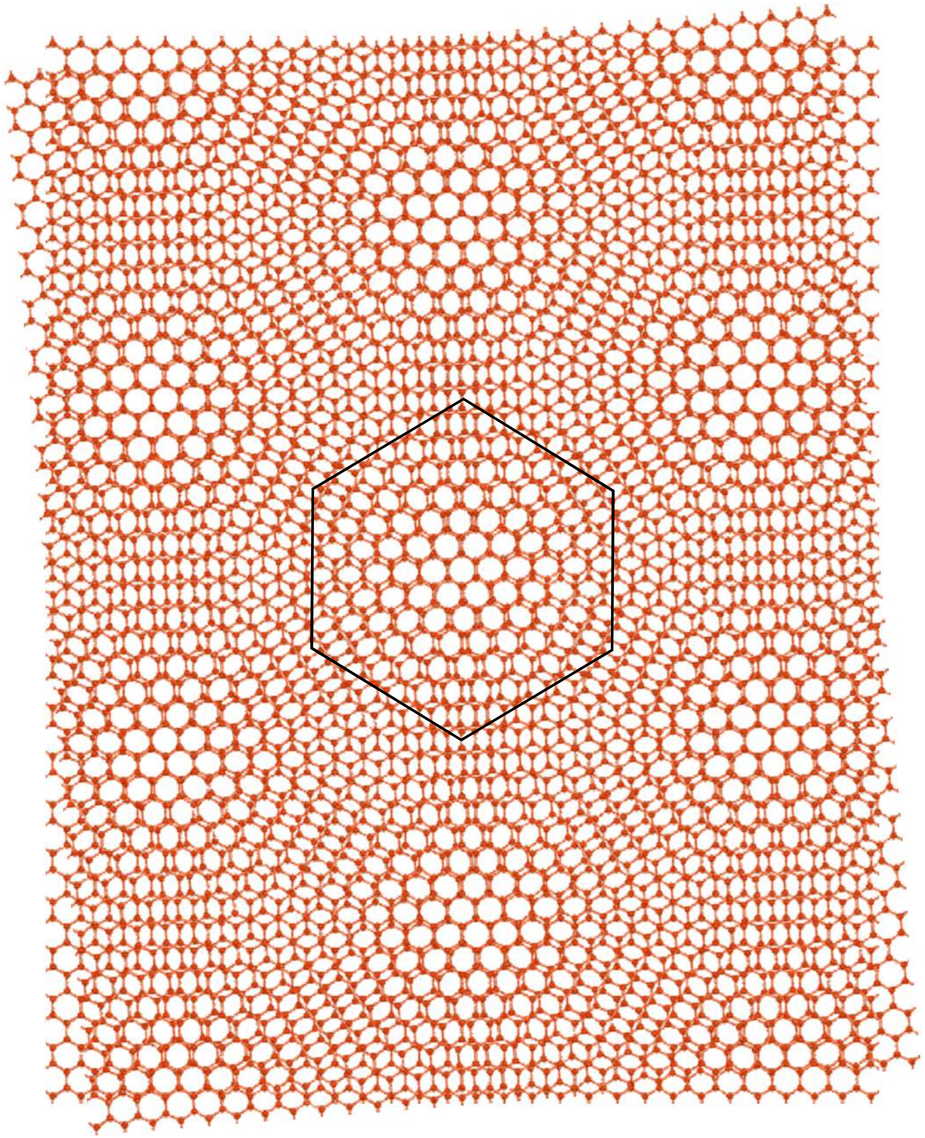

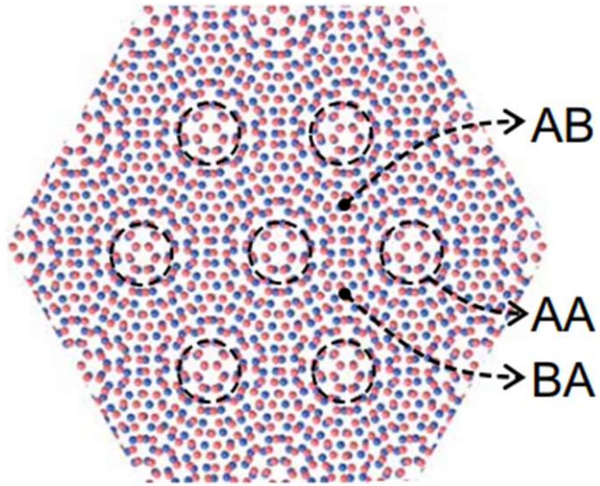

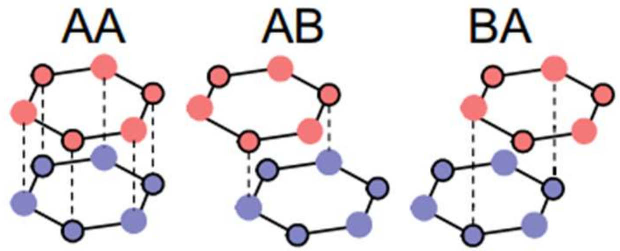

The Magic of Two-Dimensional Materials : Eva Andrei

(a)

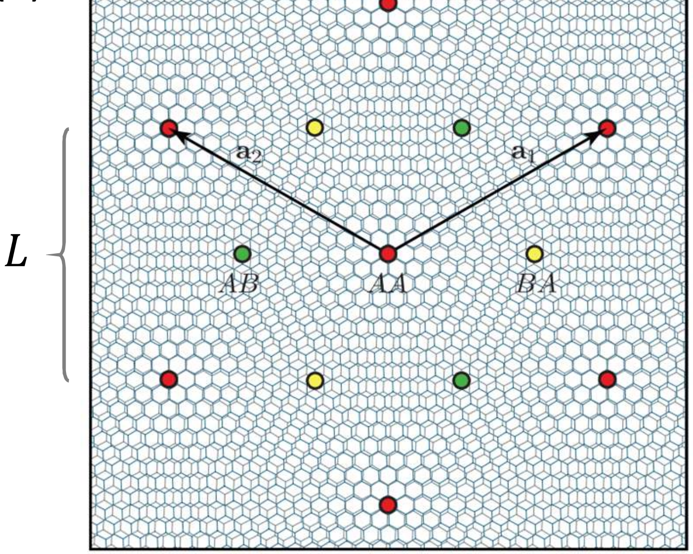

$$L = \frac{a}{2\sin\frac{\theta}{2}}$$

(b)

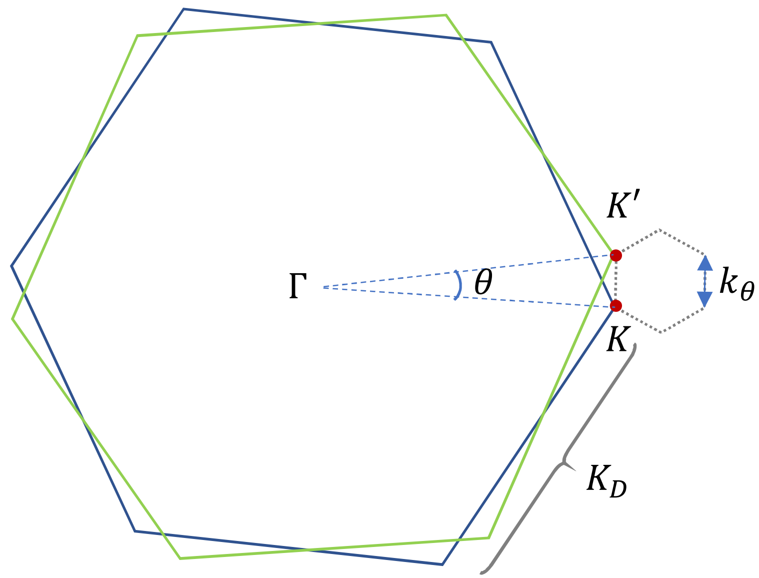

$$k_\theta = 2K_D \sin\frac{\theta}{2}$$

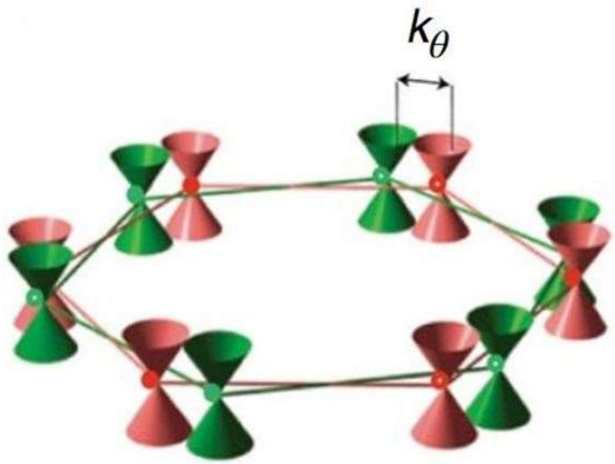

Van Hove singularity (Li et al, Nat Phys 2010)

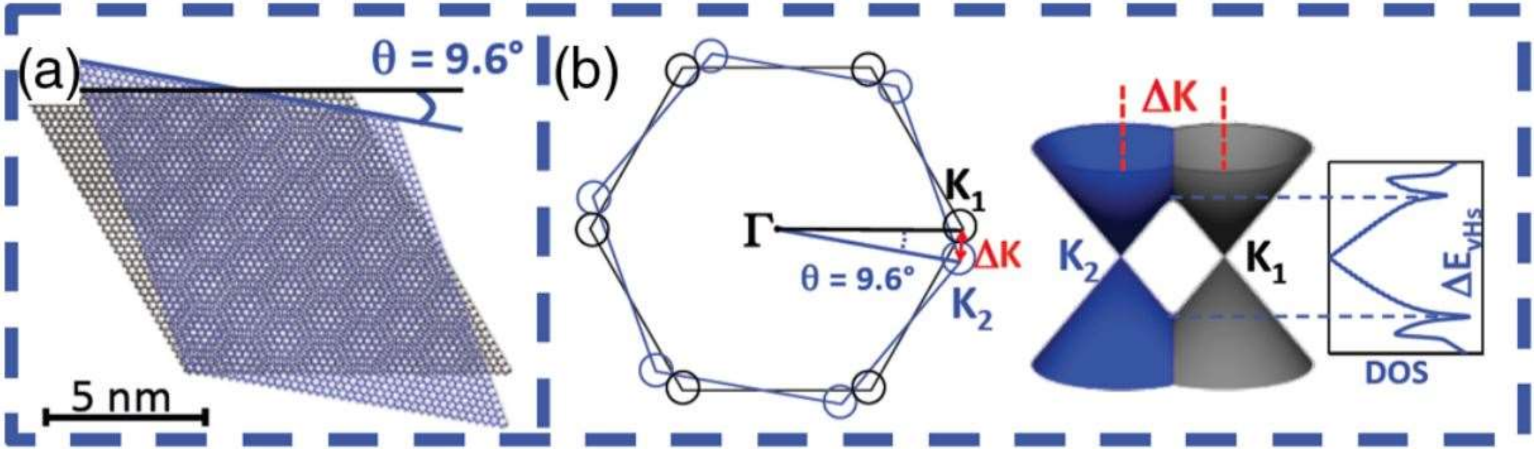

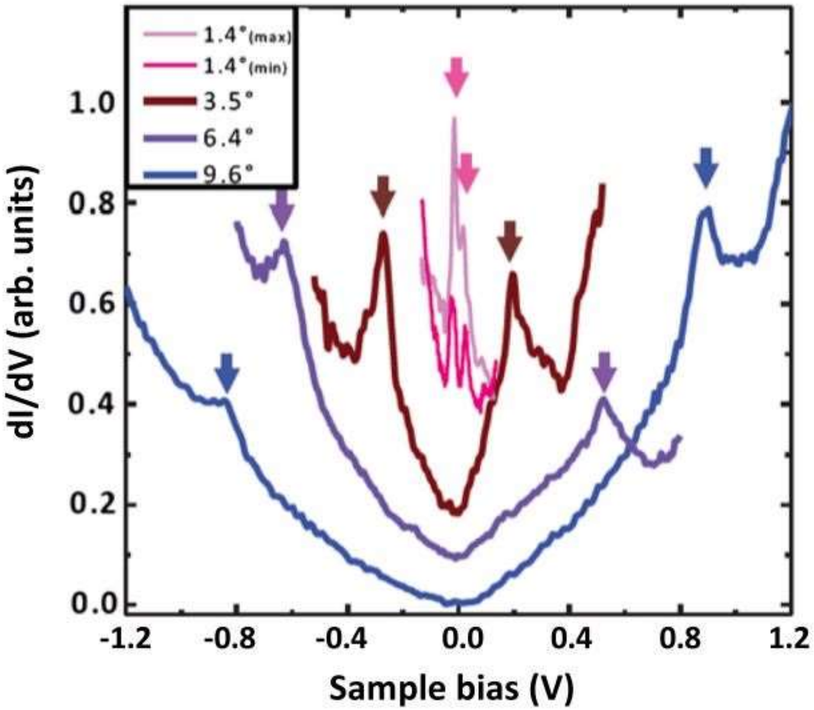

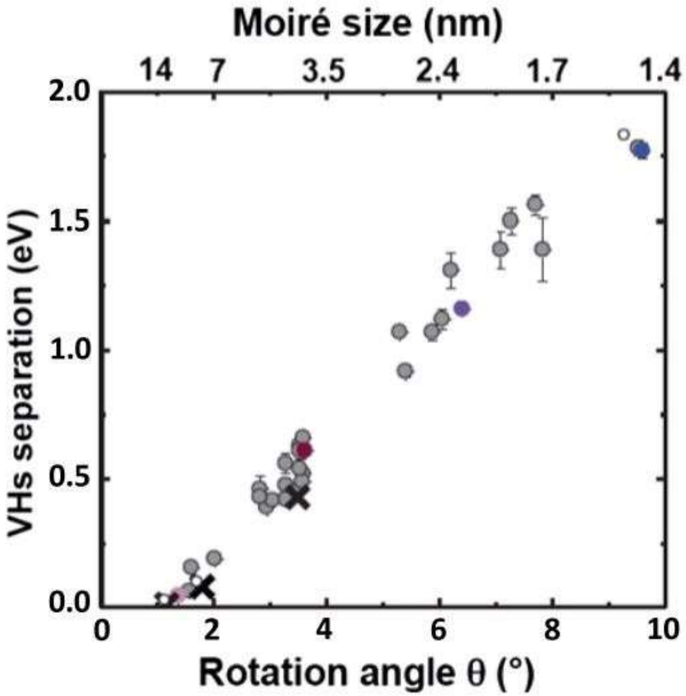

Brihuega et al, PRL 2012

Predicted magic angle for flat band (Bistritzer and MacDonald PNAS 2011)

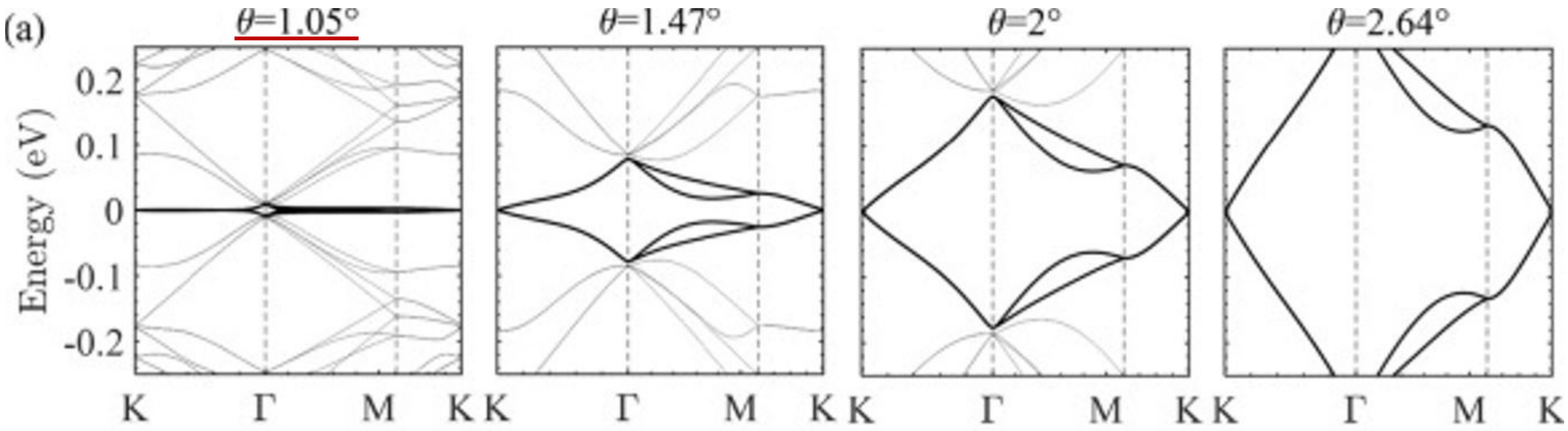

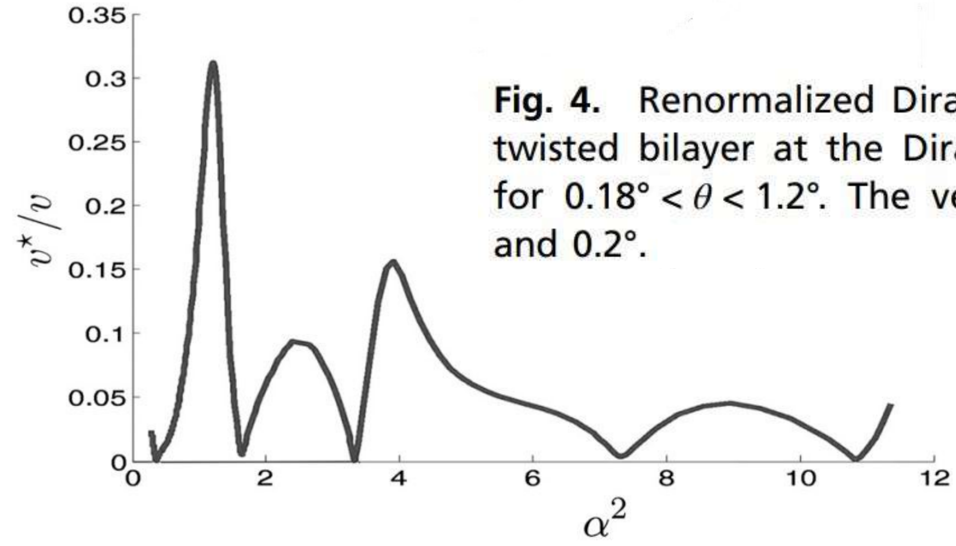

Fig. 4. Renormalized Dirac-point band velocity. The band velocity of the twisted bilayer at the Dirac point $v^\star$ is plotted vs. α^2, where $\alpha = w/vk_\theta$ for $0.18° < \theta < 1.2°$. The velocity vanishes for $\theta \approx 1.05°$, 0.5°, 0.35°, 0.24°, and 0.2°.

Flat band condition

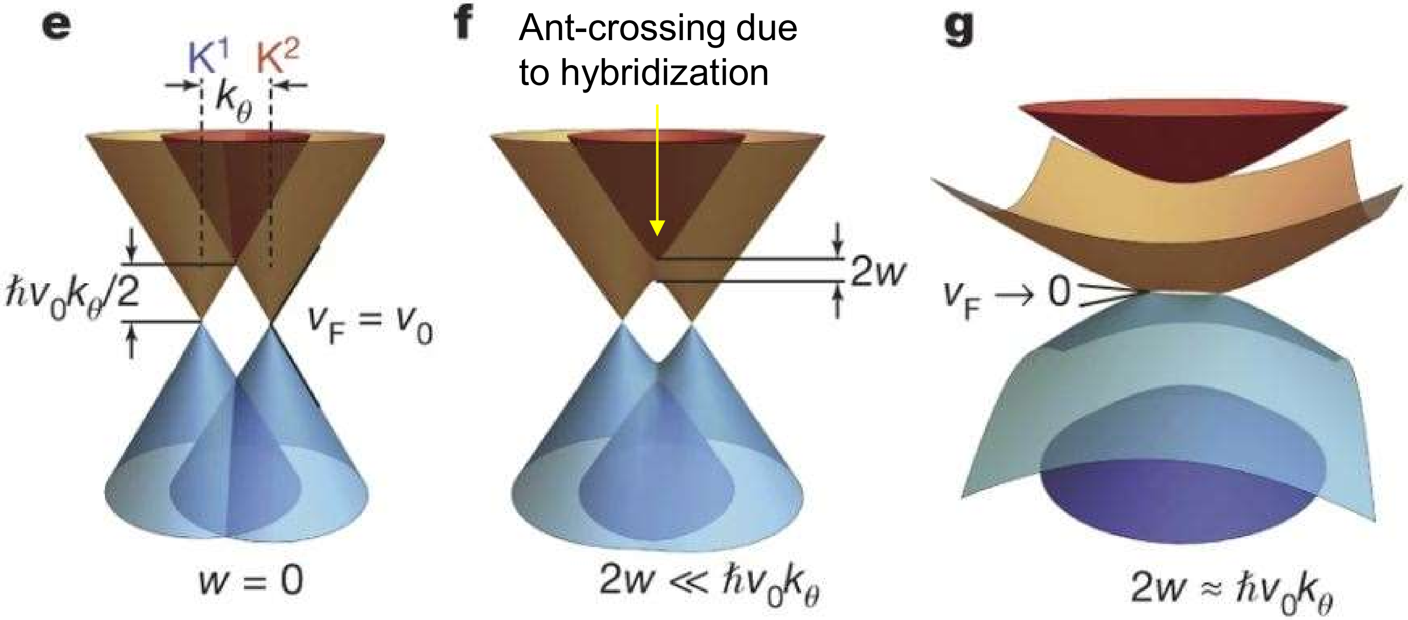

$$\hbar v_F \frac{k_\theta}{2} = w \simeq 0.1 \text{ eV}$$

$$\hbar v_F = \frac{3}{2} a t_1$$

$$k_\theta = 2K \sin\frac{\theta}{2}$$

$$K = \frac{4\pi}{3\sqrt{3}a}$$

$$\Rightarrow \quad \theta = \frac{\sqrt{3}w}{\pi t_1} \simeq 1.17^o$$

Why are we interested in flat (narrow) bands?

- Flat band dispersion → small kinetic energy → enhanced correlations

$E = \cancel{K} + U$

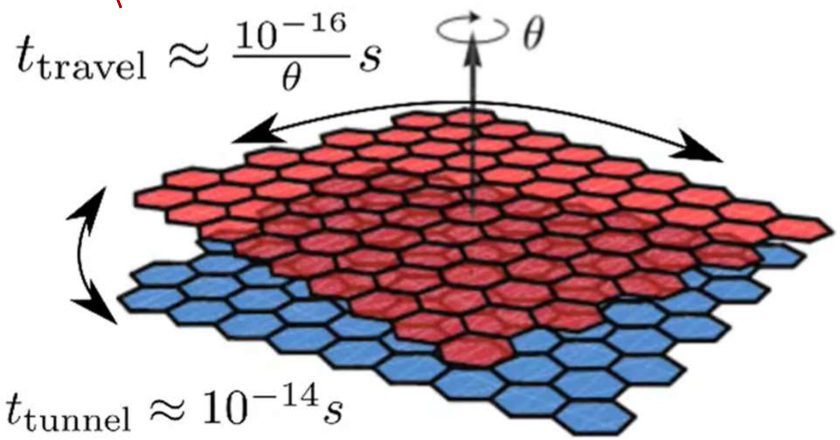

- Mott insulator
- CDW (nematic order)
- Superconductivity
- Chern insulator
- Fractional Chern insulator
- Ferromagnetism

…

Systems with flat bands

- Landau levels (Quantum Hall systems), need B field.
- Twisted bilayer (trilayer…) graphene
- Twisted bilayer TMD or other superstructures
- Heavy fermion materials
- …

Magic-Angle Graphene Superlattices: Pablo Jarillo-Herrero

Energy scales in Magic Angle TBG

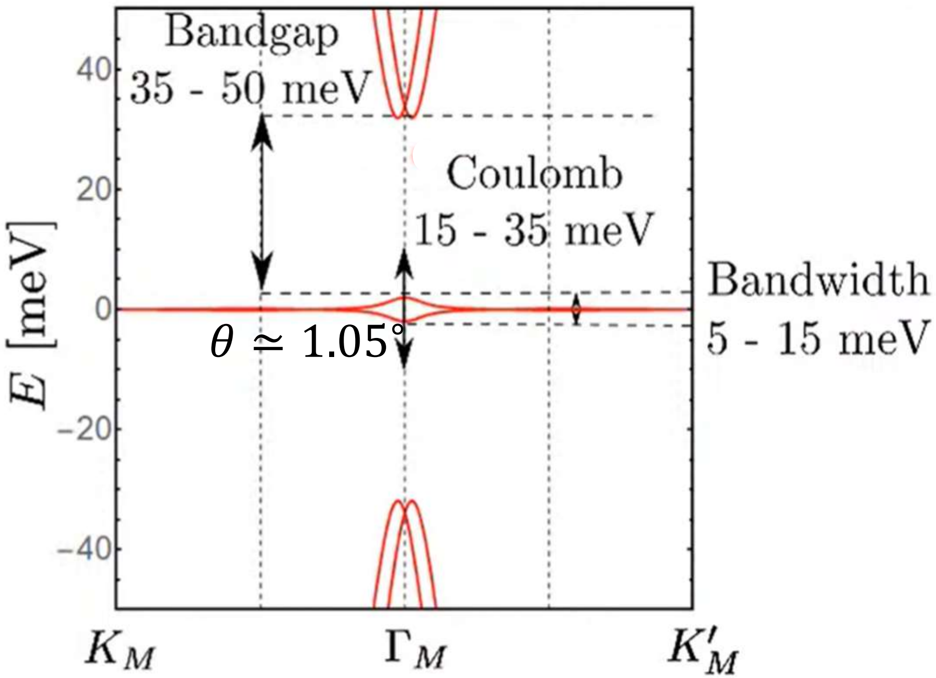

- Without spin, there are 2+2 nearly flat electron+hole bands.
- With spin, there are 4+4 bands, and the range of filling factor ν=[-4,4]

(ν = number of carriers/moire cell)

Red: fully occupied   Green: fully empty
(under flat-band condition)

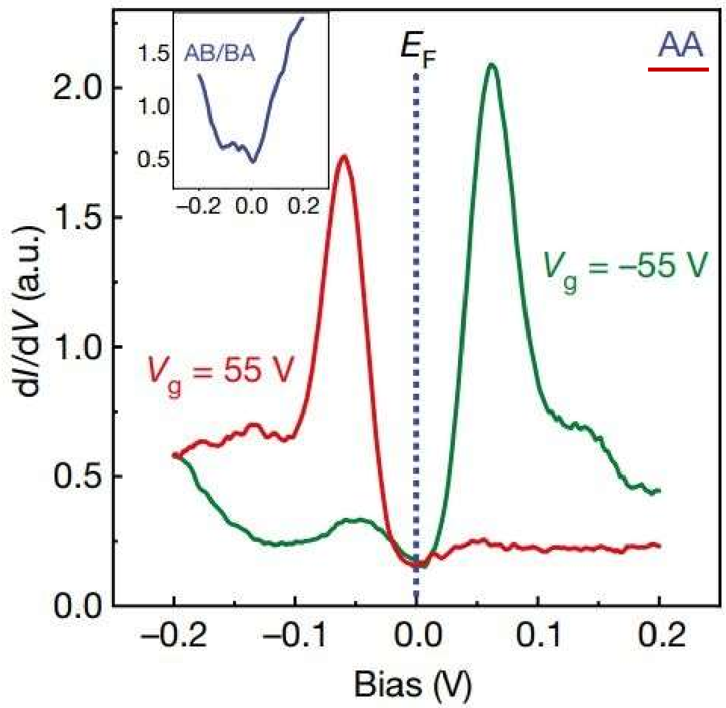

Near half-filled regime

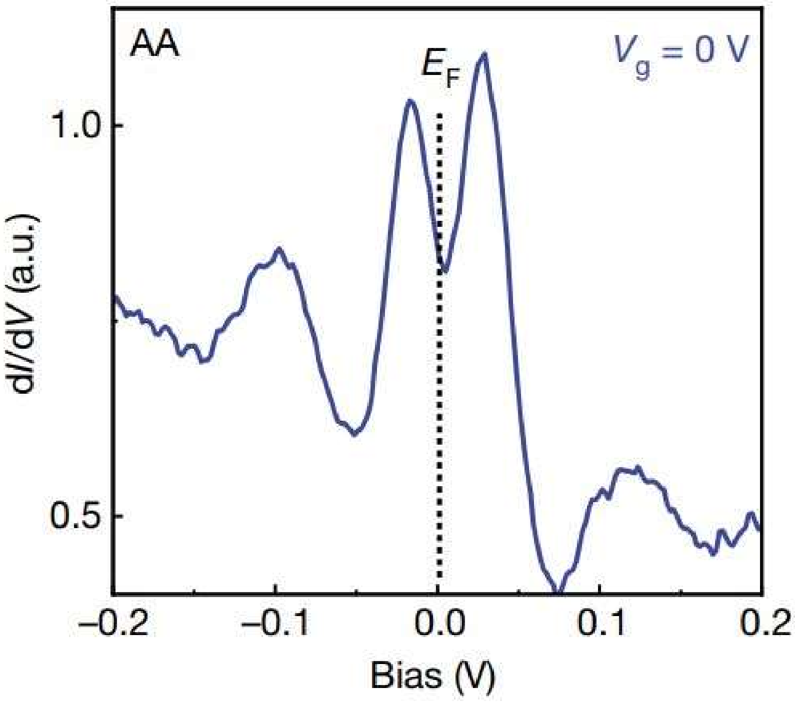

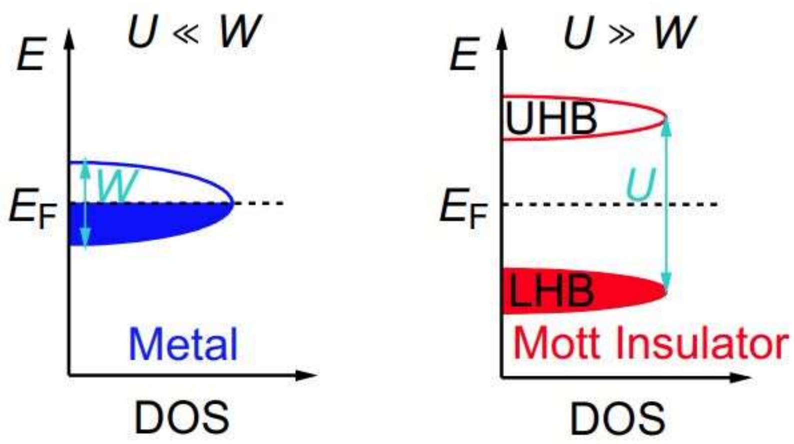

Interaction-induced energy gap

(~ Mott insulator)

Jiang et al, Nature 2019

Superconductivity in TBG (Tc ~ 1.7 K)

Cao et al, Nature 2018

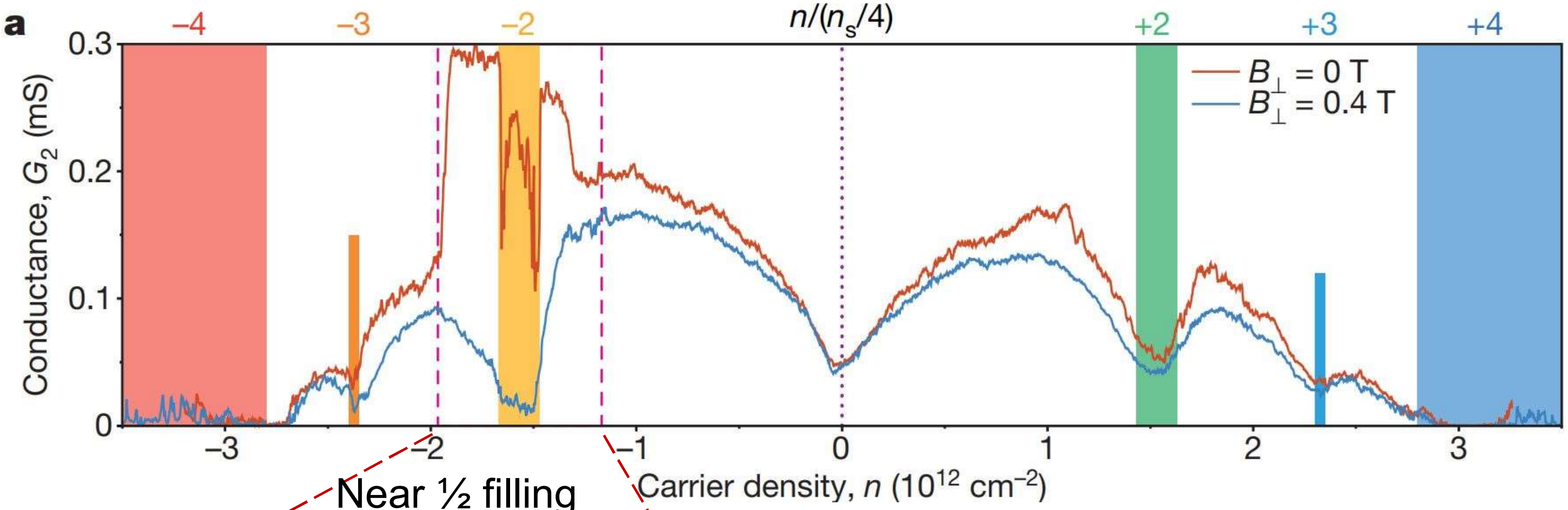

Near ½ filling

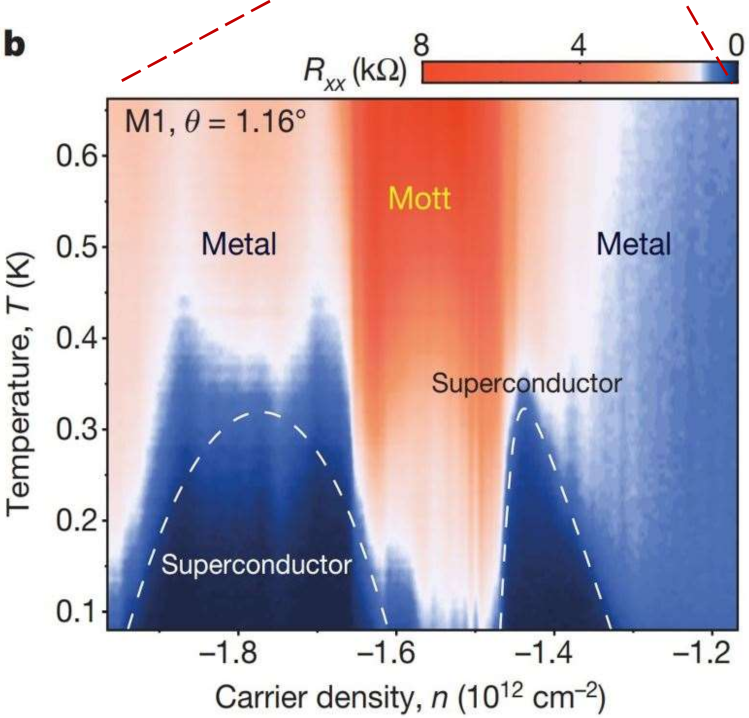

Electrically tunable

High-Tc superconductivity

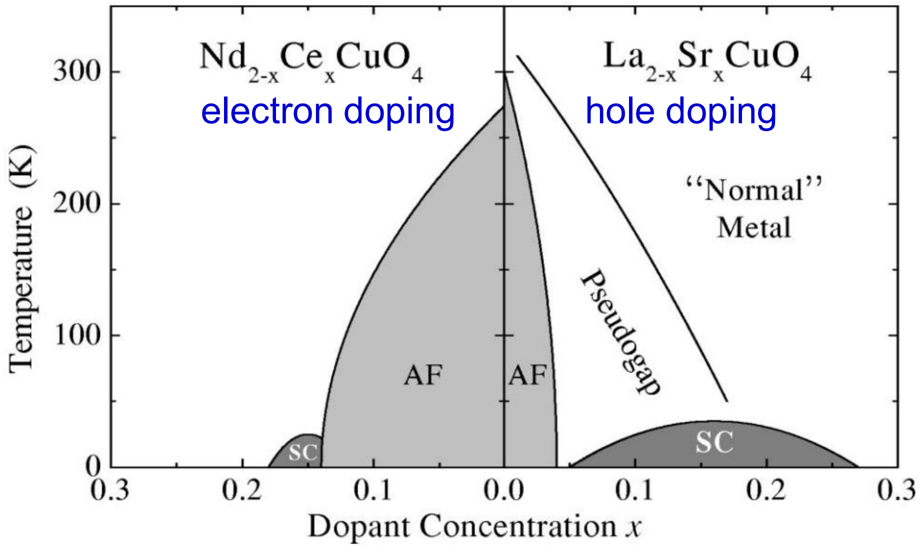

Collective data from many experiments

Damascelli et al, RMP 2003

Quantized anomalous Hall effect in twisted bilayer graphene at 1.6 K

Serlin et al, Science 2020

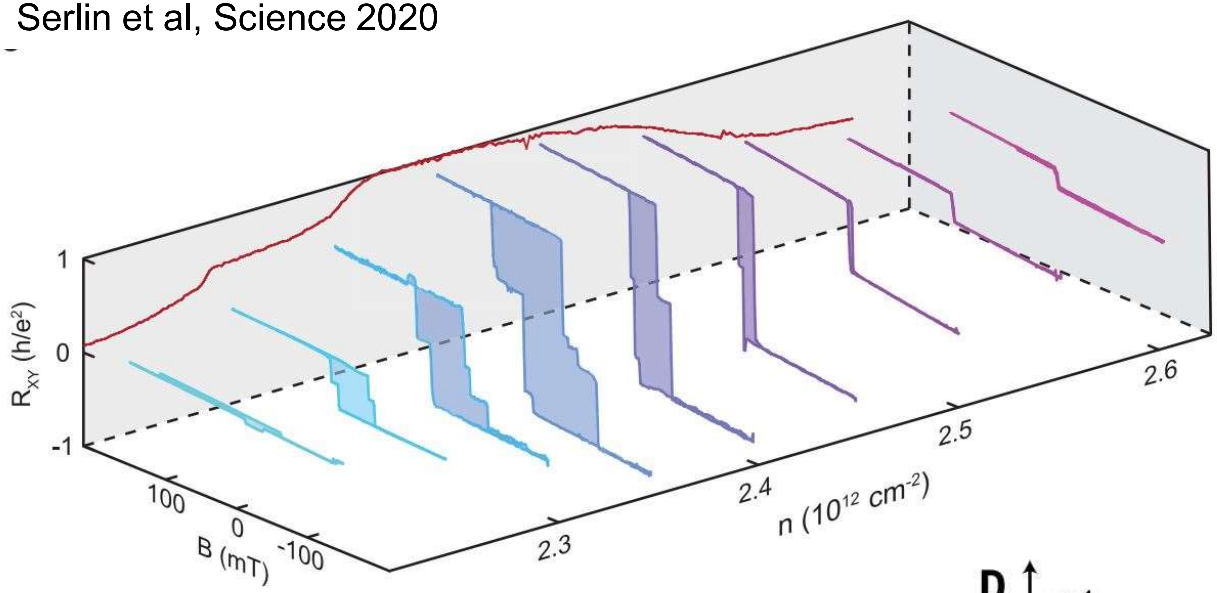

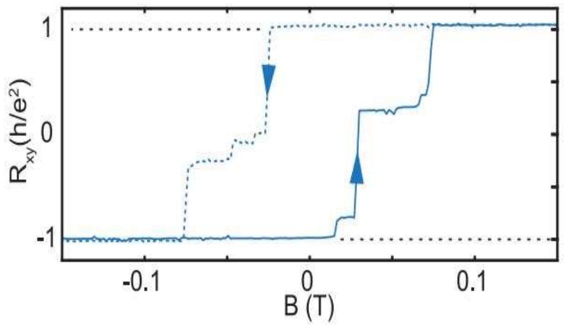

Schematic band structure at full filling of a moiré unit cell (ν = 4) and ν = 3

Spontaneous spin and valley polarization

The topology of |C|=1 flat band ~ that of LLs

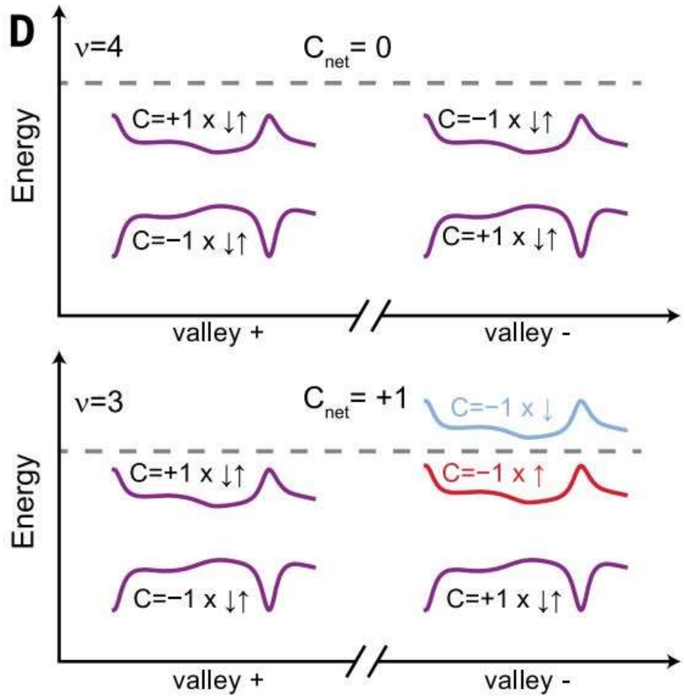

Table 1 | Advantages offered by moiré superlattices compared with atomic lattices in the exploration of Berry physics

Parameter	Atomic 2D lattices	Moiré 2D lattices
Lattice period l	~0.1 nm	~10 nm
Bandgap Δ	~1 eV	~10 meV
Berry curvature of gapped graphene $\Omega^z(k) = \frac{(\hbar v_F)^2 \Delta}{2[(\hbar v_F k)^2 + \Delta^2]^{3/2}}$ At $k = 0 : \frac{\Omega^z(k=0)}{(\hbar v_F)^2} = \frac{1}{2\Delta^2}$	$\sim\frac{1}{1\,\text{eV}^2}$	$\sim\frac{1}{0.01\,\text{eV}^2}$
Berry curvature $[r_i, r_j] = i\varepsilon^{ijk}\Omega(k) \Rightarrow \Omega(k) \sim l^2$	~(0.1 nm)^2	~(10 nm)^2
Berry curvature dipole BCD $\hbar \propto \int f(E)\frac{\partial\Omega(k)}{\partial k}\mathrm{d}k$ BCD in 2D ~$1/k \sim l$	~0.1 nm	~10 nm
Tunable gap	Some, such as bilayer graphene	Yes, mostly
Tunable Fermi velocity	No	Yes
Tunable Berry curvature dipole	Yes, in WTe_2	Yes, with electric field and density of carriers
Tunable valley Chern transitions	No	Yes

Adak et al, Nat Rev Materials 2024

Highly tunable: Twist angle, gate bias, strain … etc

Twistronics (Carr PRB 2017)

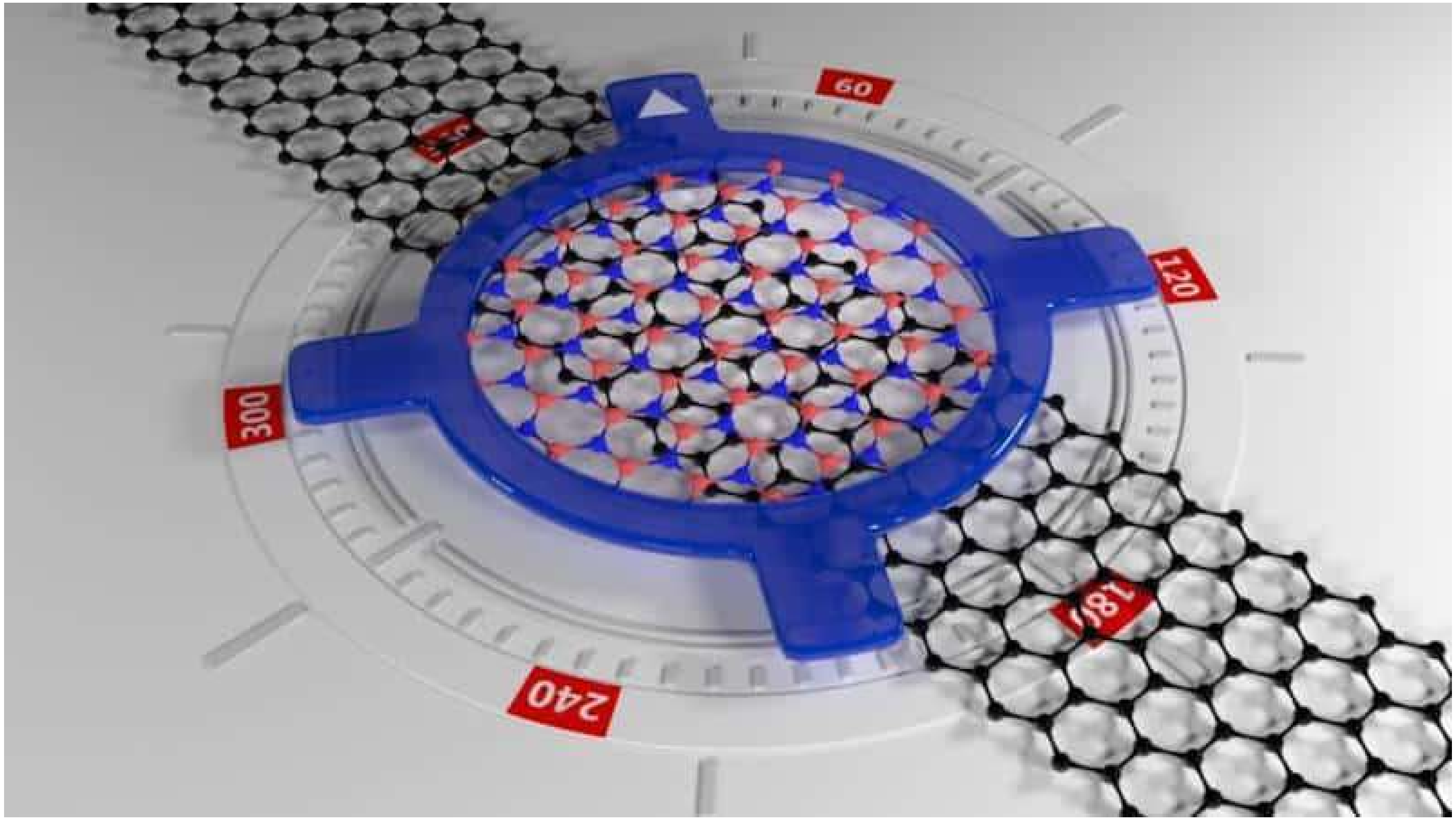

See Twistronics@wikipedia

Twisted bilayer graphene

- Integer quantum Hall effect (Lee et al, Phys Rev Lett 2011)
- Hofstadter butterfly (Hunt et al, Science 2013)
- Fractal quantum Hall effect (Dean et al, Nature 2013)
- Fractional quantum Hall effect (Wang et al, Science 2015)
- Insulating state at half filling (Cao et al, Nature 2018)
- Superconducting states (Cao et al, Nature 2018)
- Orbital ferromagnetism (Sharpe et al, Science 2019)
- Quantum AHE (Serlin et al, Science 2019)
- Chern insulators (Nuckolls et al, Nature 2020)
- Fractional Chern insulator (Xie et al, Nature 2021)
- BCD, nonliner Hall effect (Sinha et al, 2204.02848)
- …

A platform for rich physics

Correlated Insulators
(MATBG, ABC/hBN, Twisted Bi-Bi,
TMD moiré, etc)

Superconductivity
(MATBG, MATTG, MATNG, 2ATTG
signatures in others)

Topological Phases
(MATNG, MATBG/hBN,
ABC/hBN, Twisted Bi-Bi,
Twisted Mono-Bi, etc))

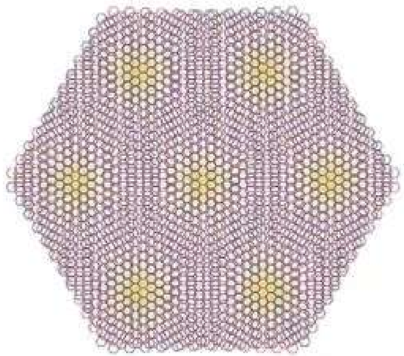

Magnetism
(MATBG/hBN, ABC/hBN,
Twisted Mono-Bi)

Nematicity
(MATBG, TMD moiré)

Moiré Ferroelectricity
(Twisted BN/BN, TMD/TMD,
BLG/BN)

Strange Metal (MATBG, MATTG)
Generalized Wigner Crystals (TMD/TMD)
Excitonic Insulators (TMD/TMD)
Moiré Quasicrystals (2ATTG)

⋮

From Pablo Jarillo-Herrero’s talk @ Aspen 2023

Beyond graphene layers

With hundres of 2D van der Waals materials… we have barely started to scratch the surface of the moiré quantum matter universe…

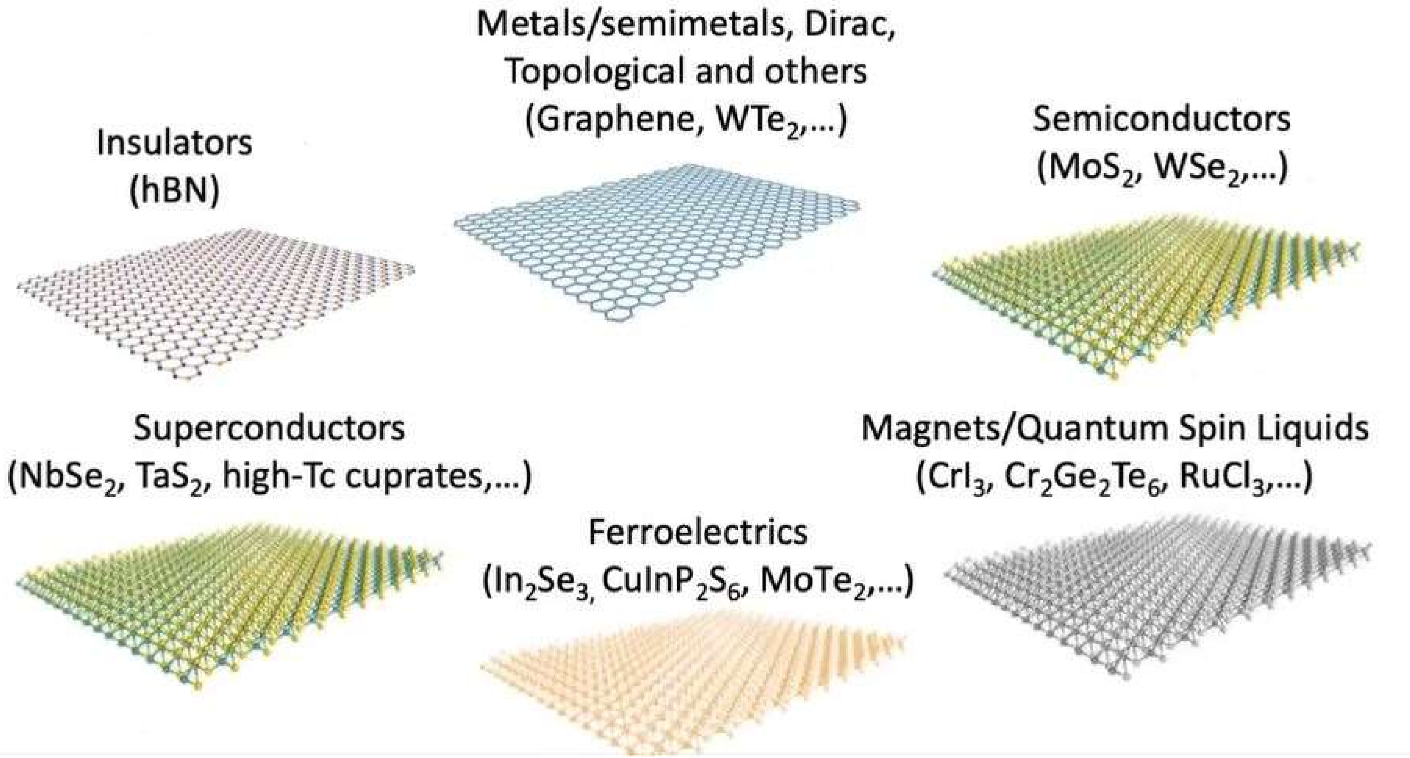

From Pablo Jarillo-Herrero’s talk @ Aspen 2023

$$\hat{H} = \hat{H}_1 + \hat{H}_2 + \hat{H}_{12}$$

$$\hat{H}_{12} = \sum_{\mathbf{R},\mathbf{R}'} \sum_{\alpha,\beta} t_\perp \left(\mathbf{R}_\alpha - \mathbf{R}'_\beta\right) c^\dagger(\mathbf{R}_\alpha) c(\mathbf{R}'_\beta) + h.c.$$

$$\hat{H}_{12} = \sum_{\mathbf{k},\mathbf{k}'} \sum_{\alpha,\beta} \left(T^{\alpha\beta}_{\mathbf{k}\mathbf{k}'} c^\dagger_{\alpha\mathbf{k}} c_{\beta\mathbf{k}'} + T^{\beta\alpha}_{\mathbf{k}'\mathbf{k}} c^\dagger_{\beta\mathbf{k}'} c_{\alpha\mathbf{k}} \right)$$

$$\begin{aligned} T^{\alpha\beta}_{\mathbf{k}\mathbf{k}'} &= T_{\alpha\beta}(Q_0)\delta_{\mathbf{k},\mathbf{k}'} + T_{\alpha\beta}(Q_1)\delta_{\mathbf{k}-\mathbf{G}_1,\mathbf{k}'-\mathbf{G}'_1} \\ &+ T_{\alpha\beta}(Q_2)\delta_{\mathbf{k}+\mathbf{G}_2,\mathbf{k}'+\mathbf{G}'_2}, \end{aligned}$$

$$\boxed{\begin{aligned} \mathbf{R}_\alpha &= n_1\mathbf{a}_1 + n_2\mathbf{a}_2 + \boldsymbol{\delta}_\alpha \\ &= \mathbf{R} + \boldsymbol{\delta}_\alpha, \;\; \alpha = A, B \\ \mathbf{R}'_\beta &= \mathbf{R}' + \boldsymbol{\delta}'_\beta + \mathbf{d}, \;\; \beta = A, B \\ &= \mathsf{M}\left(\mathbf{R} + \boldsymbol{\delta}_\beta\right) \end{aligned}}$$

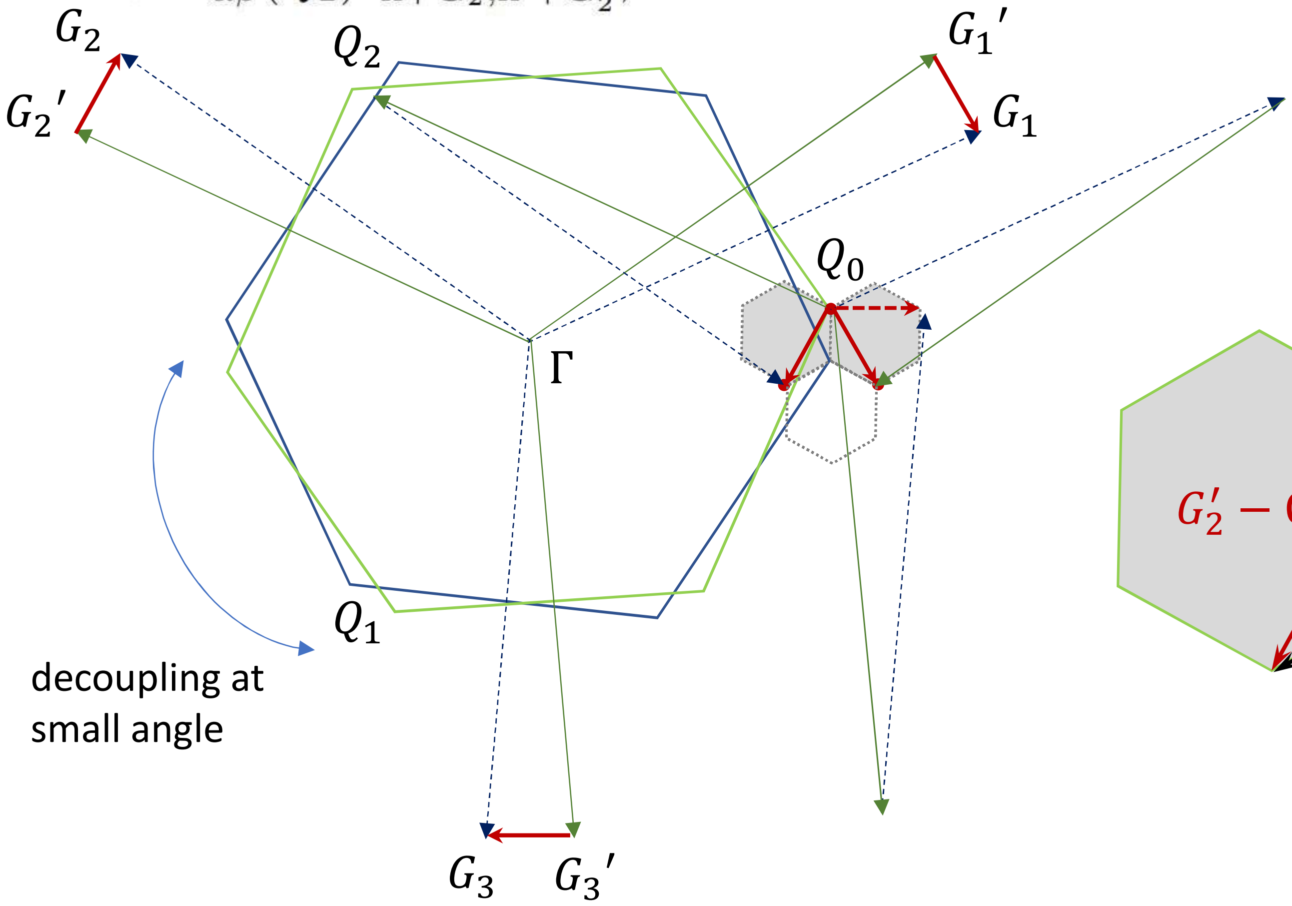

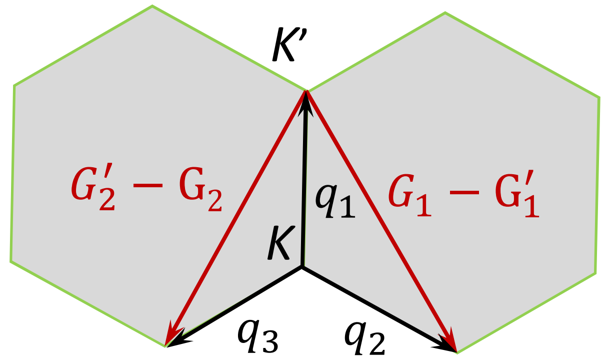

$$
\begin{aligned}
\mathsf{T}_{\mathbf{k}\mathbf{k}'} &= \mathsf{T}(Q_0)\delta_{\mathbf{k},\mathbf{k}'} + \mathsf{T}(Q_1)\delta_{\mathbf{k}-\mathbf{G}_1,\mathbf{k}'-\mathbf{G}'_1} \\
&+ \mathsf{T}(Q_2)\delta_{\mathbf{k}+\mathbf{G}_2,\mathbf{k}'+\mathbf{G}'_2}.
\end{aligned}
$$

$$
\begin{aligned}
\mathsf{T}(Q_0) &= t\begin{pmatrix} \gamma & 1 \\ 1 & \gamma \end{pmatrix}, \\
\mathsf{T}(Q_1) &= t\begin{pmatrix} \gamma & e^{i2\pi/3} \\ e^{-i2\pi/3} & \gamma \end{pmatrix} \\
\mathsf{T}(Q_2) &= t\begin{pmatrix} \gamma & e^{-i2\pi/3} \\ e^{i2\pi/3} & \gamma \end{pmatrix}
\end{aligned}
$$

$$
t \equiv t_\perp^{AB}(Q_\ell), \quad \gamma \equiv \frac{t_\perp^{AA}}{t_\perp^{AB}} \simeq 0.8
$$

$$
\begin{pmatrix} \hbar v_F \boldsymbol{\sigma}^{-\frac{\theta}{2}} \cdot (\mathbf{k}-\mathbf{K}) & \mathsf{T}_{\mathbf{k}\mathbf{k}'} \\ \mathsf{T}^\dagger_{\mathbf{k}'\mathbf{k}} & \hbar v_F \boldsymbol{\sigma}^{+\frac{\theta}{2}} \cdot (\mathbf{k}'-\mathbf{K}') \end{pmatrix} \begin{pmatrix} \psi_1(\mathbf{k}) \\ \psi_2(\mathbf{k}') \end{pmatrix} = \varepsilon \begin{pmatrix} \psi_1(\mathbf{k}) \\ \psi_2(\mathbf{k}') \end{pmatrix}
$$

$\hbar v_F \simeq 550$ meV $\cdot$ nm

$t \simeq 100$ meV

$$
\boldsymbol{\sigma}^{\pm\frac{\theta}{2}} \equiv U^\dagger\left(\pm\frac{\theta}{2}\right)\boldsymbol{\sigma} U\left(\pm\frac{\theta}{2}\right)
$$